Aust. J. Phys., 1980, **33**, 691–717

The Low-lying Levels of ^{13}C and ^{13}N

F. C. Barker and Nasima Ferdous

Department of Theoretical Physics, Research School of Physical Sciences, Australian National University, P.O. Box 4, Canberra, A.C.T. 2600.

Abstract

An attempt is made to give a consistent account of observed properties of the low-lying levels of the mirror nuclei ^{13}C and ^{13}N. In the first stage of this analysis, least squares fits of the data are made using R-matrix formulae in the one- and two-level approximations; in the second stage, the resultant parameter values are compared with shell model predictions. Fitted properties include level widths, neutron scattering data, E1 radiative widths and E1 capture cross sections. The R-matrix formulae include external contributions to the E1 transition matrix elements, calculated using wavefunctions with the correct asymptotic forms. Acceptable fits are obtained for channel radii in the range 4–6 fm, with the lower values preferred. The parameter values obtained in these fits agree with shell model predictions, except for quantities involving the $\frac{3}{2}^-$ levels. Level displacement energies are calculated from the fitted parameter values. A reasonable account is given of two notable asymmetries between ^{13}C and ^{13}N—the very different excitation energies of the first excited states and the very different strengths of the E1 decays of these states.

1. Introduction

Nearly 30 years ago, Thomas (1952) summarized the properties then known of the low-lying $\frac{1}{2}^-$, $\frac{1}{2}^+$, $\frac{3}{2}^-$ and $\frac{5}{2}^+$ levels of the mirror nuclei ^{13}C and ^{13}N, and used the nuclear reaction theories of Wigner and others to give a consistent account of them. Since that time, more experimental data concerning these levels and detailed shell model descriptions of them have become available. Some of this new information is not consistent with Thomas's assumptions or predictions. It thus seems timely to reanalyse the available data and compare the resultant parameter values with shell model calculations, to see if a consistent overall description is possible.

The data fitted by Thomas (1952) included level energy displacements and widths, and nucleon scattering and capture cross sections. Thomas mostly used a one-channel approximation, describing the ^{13}C and ^{13}N levels as a single neutron or proton outside a ^{12}C ground-state core. Except for the $\frac{1}{2}^+$ levels, he also used a one-level approximation. The one-level approximation was not sufficient to describe the data on the $\frac{1}{2}^+$ levels, and Thomas included the effect of higher $\frac{1}{2}^+$ levels by using the representation of Feshbach *et al.* (1947) for the logarithmic derivative function.

We prefer to use the formalism of standard R-matrix theory (Lane and Thomas 1958) rather than that of Feshbach *et al.* This enables the description to be made in terms of constant parameters (eigenenergies E_λ and reduced width amplitudes $\gamma_{\lambda c}$) instead of an energy dependent quantity $Z(E)$, which is only restricted to be a monotonic increasing function of E although it is anticipated to have a fairly smooth energy dependence. The values of these and other constant parameters (the internal transition moments $\mathscr{M}_{if}$ between states i and f) required to fit the experimental data can then be compared with values calculated from the nuclear shell model. Thus the R-matrix treatment separates the problem of relating experimental data and models into two parts:

$$\text{data} \leftrightarrow \text{parameters}, \qquad \text{parameters} \leftrightarrow \text{models}.$$

In practice the separation may not be complete, since restrictions on the number of parameters used to fit the data may be based on model arguments, or the values of some parameters that are not well determined by the data may be taken from model calculations.

In Thomas's best fit to the available data, the reduced width for the channel ^{12}C ground state + p-wave nucleon was greater by a factor of about 2 in the excited $\frac{3}{2}^-$ states of the $A = 13$ nuclei than in the $\frac{1}{2}^-$ ground states. Recent experimental values, however, as well as shell model calculations, suggest that the factor should be only about $\frac{1}{3}$. Also, the width of the $\frac{1}{2}^+$ first excited state of ^{13}C has recently been measured and is about $\frac{1}{4}$ of the value predicted by Thomas's parameters. This small width makes the strength of the $\frac{1}{2}^+ \to \frac{1}{2}^-$ E1 transition in ^{13}C less than one-half the corresponding strength in ^{13}N, although charge-symmetric forces would require such strengths in mirror nuclei to be equal. Shell model descriptions do not support the one-channel approximation for some of the low-lying levels of ^{13}C and ^{13}N, and it seems that a more general description is needed to explain the different strengths of the $\frac{1}{2}^+ \to \frac{1}{2}^-$ transitions.

Another obvious evidence of departure from charge symmetry is the 720 keV difference in energies of the $\frac{1}{2}^+$ first excited states of ^{13}C and ^{13}N, the original and most pronounced example of the Thomas–Ehrman shift. Thomas calculated only two contributions to such level displacements, namely those from the different external wavefunctions in the mirror nuclei and from the electromagnetic spin–orbit interaction; we include many other contributions and also do not make the one-channel approximation. Thomas used his fits to the level displacements in obtaining best values of the level parameters; we obtain the level parameters by fitting other data and use them to predict the level displacements. We do not attempt to fit the level displacements exactly since we do not include the effects of any charge-symmetry-breaking potential in the nuclear forces.

The experimental data that are fitted in order to determine values of the parameters E_λ, $\gamma_{\lambda c}$ and $\mathscr{M}_{if}$ are given in the next section. We have not included other data that do not yield direct information about these parameters, such as M1 matrix elements and log ft values, which are discussed by Cohen and Kurath (1965). The relevant R-matrix formulae are given in Section 3, and fits to the data are made in Section 4. In Section 5 the resultant parameter values are compared with shell model values and with values deduced from other experimental data. Coulomb displacement energies are calculated and compared with experimental values in Section 6. A discussion of these results and comments on earlier partial fits to the data are given in Section 7.

2. Experimental Data

Experimental values of quantities relating to the lowest four levels in each of ^{13}C and ^{13}N are taken from Ajzenberg-Selove (1976), unless another reference is given.

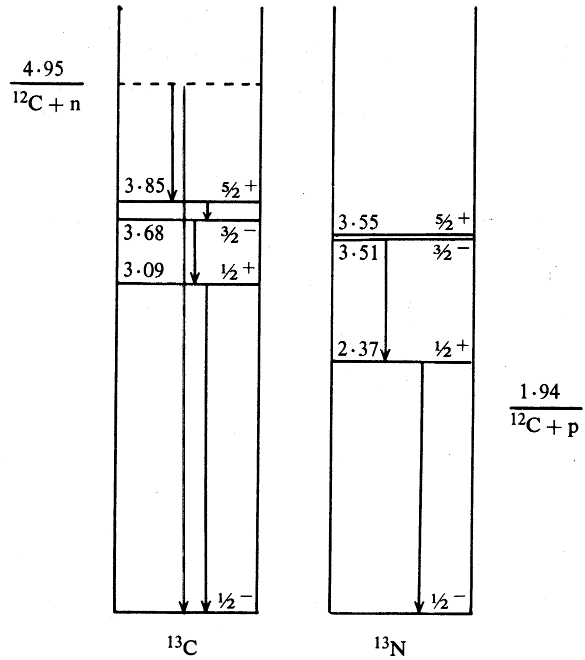

Fig. 1. Low-lying energy levels of ^{13}C and ^{13}N and the E1 transitions between them.

Table 1. Values of quantities related to lowest levels of ^{13}C and ^{13}N

Relevant J^{π} value	Quantity	Thomas (1952)	Adopted value	Best fit a = 5 fm
$\frac{1}{2}^{+}$	E_b (MeV)	$-1·85$	$-1·858 \pm 0·001$	$-1·858^{A}$
	E_r (MeV)	0·42	$0·421 \pm 0·001$	$0·421^{A}$
	a_s (fm)	6·11	$6·142 \pm 0·0012$	$6·142^{A}$
	r_0 (fm)	2·9–3·6	$3·42 \pm 0·1$	$3·42^{A}$
	$\Gamma^{o}(^{13}\mathrm{N})$ (keV)	35	33 ± 2	33^{A}
$\frac{1}{2}^{+} \to \frac{1}{2}^{-}$	$\Gamma_{\gamma}^{o}(^{13}\mathrm{C})$ (eV)		$0·43 \pm 0·04$	0·472
	$\sigma_{n\gamma}$(thermal) (mb)	1·8–3·5	$2·31 \pm 0·21$	2·36
	$\sigma_{p\gamma}(E_r)$ (μb)	125 ± 15	102 ± 8	97·1
	$\sigma_{p\gamma}(E_p = 120$ keV) (nb)	$0·61 \pm 0·09$	$0·61 \pm 0·09$	0·607
	$\sigma_{p\gamma}(E_p = 604$ keV) (μb)		$2·17 \pm 0·19$	2·03
$\frac{3}{2}^{-}$	$\Gamma^{o}(^{13}\mathrm{N})$ (keV)	70 ± 10	60 ± 5	
$\frac{3}{2}^{-} \leftrightarrow \frac{1}{2}^{+}$	$\Gamma_{\gamma}^{o}(^{13}\mathrm{C})$ (meV)		$6·6 \pm 1·4$	6·82
	$\sigma_{n\gamma}$(thermal) (mb)		$1·09 \pm 0·10$	1·09
	$\Gamma_{\gamma}^{o}(^{13}\mathrm{N})$ (eV)		$0·054 \pm 0·014$	0·0505
$\frac{5}{2}^{+}$	$\Gamma^{o}(^{13}\mathrm{N})$ (keV)	40	52 ± 6	52^{A}
$\frac{5}{2}^{+} \to \frac{3}{2}^{-}$	$\Gamma_{\gamma}^{o}(^{13}\mathrm{C})$ (meV)		$0·019 \pm 0·001$	$0·019^{A}$

^{A} Exact fit.

The relevant part of the energy-level diagrams of ^{13}C and ^{13}N is given in Fig. 1. This shows the energies of the levels and the E1 transitions that we consider.

Values of the fitted quantities are collected in Table 1. These are grouped according to the J^{π} values of the levels involved. The values that Thomas (1952) used are given, along with the presently adopted values and the values obtained in our best fits. Of the quantities fitted, E_b and E_r are the energies of the ^{13}C and $^{13}N\ \frac{1}{2}^+$ levels measured from the threshold of the ^{12}C ground-state channel. The scattering length a_s and effective range r_0 are obtained from the scattering of slow neutrons on ^{12}C. The Γ^o and Γ_γ^o are total and radiative widths in the c.m. system (the significance of the superscript o denoting observed width is discussed in Section 3). The $\sigma_{n\gamma}$ and $\sigma_{p\gamma}$ are integrated cross sections for the reactions $^{12}C(n,\gamma)^{13}C$ and $^{12}C(p,\gamma)^{13}N$. We comment here only on the adopted values that are not given in Ajzenberg-Selove (1976).

The adopted value of a_s comes from the measurement of Koester and Nistler (1975), who gave $a_{coh} = 6\cdot6572 \pm 0\cdot0013$ fm. In a summary of previous measurements (but not including Koester and Nistler), Lachkar (1977) gave for the total elastic scattering cross section for neutrons on ^{12}C the value (in b)

$$\sigma_T = 4\cdot725 - 3\cdot251\,E + 1\cdot316\,E^2 - 0\cdot227\,E^3\,,$$

where E is the neutron lab energy in MeV. From this one obtains $a_s = 6\cdot132$ fm and the adopted value of r_0. The uncertainty attributed to r_0 is based on the observation that Heaton *et al.* (1975) gave $r_0 = 3\cdot33$ fm. The thermal-neutron cross sections are obtained from the values of $3\cdot4 \pm 0\cdot3$ mb for the total capture cross section and $68 \pm 1\%$ for the ground-state branching ratio. Absolute values of the $^{12}C(p,\gamma)$ peak cross section have been given as $\sigma_{p\gamma}(E_r) = 120\ \mu$b (Fowler *et al.* 1948), 127 μb (Seagrave 1951, 1952) and $125 \pm 15\ \mu$b (Rolfs and Azuma 1974). Using the one-level approximation, Riess *et al.* (1968) gave $\Gamma_\gamma^o(^{13}N, \frac{1}{2}^+ \to \frac{1}{2}^-) = 0\cdot45 \pm 0\cdot05$ eV; taken with the total width value of $\Gamma^o(^{13}N, \frac{1}{2}^+) = 33$ keV, this gives $\sigma_{p\gamma}(E_r) = 92 \pm 10\ \mu$b. Rolfs and Azuma quoted Vogl (1963) as giving a value of $130 \pm 4\ \mu$b, but Vogl's error is a relative error only, and he normalized his cross section to Seagrave's absolute value. By averaging the values of Rolfs and Azuma and of Riess *et al.*, we get the adopted value given in Table 1. We also fit the $^{12}C(p,\gamma)$ cross section at $E_p = 120$ keV, which Thomas took as being representative of early low-energy measurements. Cross section measurements at higher energies by Vogl (1963) and by Rolfs and Azuma (1974) agree with each other (see Fig. 3). We fit Vogl's tabulated value at $E_p = 604$ keV, renormalized to a peak cross section of 102 μb.

Many measurements have been made of the total width of the $\frac{3}{2}^-$ level of ^{13}N. The adopted value is obtained from an average of these values, converted where necessary to the c.m. system: 68 ± 8 keV (Van Patter 1949), 65 ± 9 keV (Seagrave 1951), 53 keV* (Jackson and Galonsky 1953), 60 keV* (Armstrong *et al.* 1966), $60 \pm 2\cdot5$ keV† (Andreev *et al.* 1973), $54\cdot8 \pm 11\cdot5$ keV (Blatt *et al.* 1974) and 60 ± 3 keV (Rolfs and Azuma 1974). In order to obtain the radiative width for the $\frac{3}{2}^- \to \frac{1}{2}^+$ transition in ^{13}N, we use measured values for the peak cross section $\sigma_{p\gamma_0}(E_p = 1\cdot7$ MeV) of 35 μb (Seagrave 1952) and $37\cdot5 \pm 7\cdot5\ \mu$b (Young *et al.* 1963), and for the $\frac{3}{2}^- \to \frac{1}{2}^+$ branching ratio of $8 \pm 1\%$ (Rolfs and Azuma 1974). It may be noted that the value of $0\cdot04$ eV for $\Gamma_\gamma^o(^{13}N, \frac{3}{2}^- \to \frac{1}{2}^+)$ given by Ajzenberg-Selove (1976) is based on the assumption by Young *et al.* (1963) of a total width of the $\frac{3}{2}^-$ level of $51\cdot5$ keV (lab), corresponding to a c.m. value of $47\cdot5$ keV.

* These values of the observed width Γ^o are derived from the published values of the formal width Γ of 55 and 63 keV respectively, using relation (12) in Section 3 below.

† This is based on the assumption that the published value of $65 \pm 2\cdot7$ keV is a lab value.

Ajzenberg-Selove (1976) gives for the total width of the $\frac{5}{2}^+$ level of ^{13}N, $\Gamma^{\circ}(^{13}\mathrm{N}, \frac{5}{2}^+) = 47 \pm 7$ keV, which comes entirely from the measurement of Blatt *et al.* (1974). Armstrong *et al.* (1966) gave $\Gamma = 74$ keV, but actually used *R*-matrix formulae and varied the reduced width $\gamma^2 a$ in fitting their phase shifts. From their values $\gamma^2 a = 3{\cdot}55 \pm 0{\cdot}18$ MeV fm and $a = 4{\cdot}77$ fm, we find a formal width $\Gamma = 2P\gamma^2 = 68 \pm 3{\cdot}4$ keV (where P is the penetration factor) and an observed width $\Gamma^{\circ} = 54 \pm 2{\cdot}7$ keV. Thus, their value of 74 keV is presumably a value of the formal width. Similarly, the parameters of Jackson and Galonsky (1953) give $\Gamma^{\circ} = 46$ keV. Our adopted value is an average of these.

It is of interest to compare the strengths of corresponding E1 transitions in ^{13}C and ^{13}N. The strengths obtained from the adopted values in Table 1 are given as experimental values in Table 2. In this regard, the value of $\sigma_{\mathrm{p}\gamma}(E_{\mathrm{r}}, \frac{1}{2}^+ \to \frac{1}{2}^-)$ corresponds to $\Gamma_{\gamma}^{\circ}(^{13}\mathrm{N}, \frac{1}{2}^+ \to \frac{1}{2}^-) = 0{\cdot}50 \pm 0{\cdot}04$ eV. For charge-symmetric forces, one expects strengths of corresponding E1 transitions in mirror nuclei to be equal. Although the experimental values in Table 2 for the $\frac{3}{2}^- \to \frac{1}{2}^+$ transitions are consistent with this, those for the $\frac{1}{2}^+ \to \frac{1}{2}^-$ transitions are not, and several attempts have been made previously to explain this discrepancy. The calculated values in Table 2 correspond to our best fits.

Table 2. Comparison of E1 transition strengths in ^{13}C and ^{13}N

Values of Γ_{γ}° in Weisskopf units (1 W.u. $= 0{\cdot}376\,E_{\gamma}^3$ eV, with E_{γ} in MeV)

Transition	Experiment			Calculated[A]		
	^{13}C	^{13}N	^{13}N/^{13}C	^{13}C	^{13}N	^{13}N/^{13}C
$\frac{1}{2}^+ \to \frac{1}{2}^-$	$0{\cdot}039 \pm 0{\cdot}004$	$0{\cdot}101 \pm 0{\cdot}008$	$2{\cdot}59 \pm 0{\cdot}34$	0·043	0·096	2·26
$\frac{3}{2}^- \to \frac{1}{2}^+$	$0{\cdot}083 \pm 0{\cdot}018$	$0{\cdot}095 \pm 0{\cdot}025$	$1{\cdot}14 \pm 0{\cdot}39$	0·086	0·089	1·04
$\frac{5}{2}^+ \to \frac{3}{2}^-$	$0{\cdot}0103 \pm 0{\cdot}0005$			0·0103[B]		

[A] Best fits for channel radius $a = 5$ fm.
[B] Exact fit.

3. The *R*-matrix Formulae

Formulae and notation are taken from the paper on the *R*-matrix theory of nuclear reactions by Lane and Thomas (1958), unless otherwise noted. Only those formulae required for fitting the present data are given.

We are dealing with an energy region where for each J^{π} value there is at most one open channel, the ^{12}C ground-state channel. In extracting values of the parameters E_{λ}, $\gamma_{\lambda c}$ and $\mathscr{M}_{\mathrm{if}}$ from experimental data we assume, as did Thomas (1952), a one-channel approximation, neglecting the contribution of all other (closed) channels (except in fitting the width of the $\frac{5}{2}^-$ level of ^{13}N). We do not make a similar approximation in relating these parameter values to shell model values. The channel radius a separates the internal region ($r < a$) from the external or channel region ($r \geqslant a$). Properties of the internal region are described by an R function which, for a given J^{π}, is written $R_{\mathrm{n}}(J^{\pi}, E)$ or $R_{\mathrm{p}}(J^{\pi}, E)$, where the suffixes n and p refer to the ^{13}C and ^{13}N systems respectively, and E is the channel energy. For simplicity we drop the label J^{π} unless this could cause confusion, and we assume that $a_{\mathrm{n}} = a_{\mathrm{p}} = a$ for all J^{π}. Quantities measured experimentally are expressed in terms of the R functions and certain Coulomb functions evaluated at the channel radius (the penetration factor P, the shift factor S and the hard-sphere phase shift $-\phi$), in addition to the boundary-condition parameter B. In principle, equally good fits to the experimental data can be obtained for any choice of B and for any choice of a (provided it is greater than the range of the nuclear interaction). In practice, where a one- or two-level approximation is made, some choices of a may be better than others; the quality of fit is still independent of the choice of B, although the resultant parameter values will depend on B (Barker 1972).

For each value of $J^\pi = \frac{1}{2}^-, \frac{3}{2}^-$ and $\frac{5}{2}^+$ we assume a one-level approximation:

$$R_\mathrm{n}(E) = \gamma_{1\mathrm{n}}^2/(E_{1\mathrm{n}} - E), \qquad R_\mathrm{p}(E) = \gamma_{1\mathrm{p}}^2/(E_{1\mathrm{p}} - E). \tag{1}$$

We use $B_\mathrm{n} = S_\mathrm{n}(E_{1\mathrm{n}})$ and $B_\mathrm{p} = S_\mathrm{p}(E_{1\mathrm{p}})$ so that $E_{1\mathrm{n}}$ and $E_{1\mathrm{p}}$ are just the observed energies of the levels as obtained from Fig. 1. The $\gamma_{1\mathrm{n}}$ and $\gamma_{1\mathrm{p}}$ are treated as adjustable parameters in fitting the E1 transition probabilities.

For $J^\pi = \frac{1}{2}^+$, a one-level approximation is not sufficiently accurate as Thomas (1952) pointed out, and we assume a two-level approximation:

$$R_\mathrm{n}(E) = \frac{\gamma_{1\mathrm{n}}^2}{E_{1\mathrm{n}} - E} + \frac{\gamma_{2\mathrm{n}}^2}{E_{2\mathrm{n}} - E}, \qquad R_\mathrm{p}(E) = \frac{\gamma_{1\mathrm{p}}^2}{E_{1\mathrm{p}} - E} + \frac{\gamma_{2\mathrm{p}}^2}{E_{2\mathrm{p}} - E}. \tag{2}$$

The level 1 is associated with the low-lying $\frac{1}{2}^+$ level (at 3·088 MeV in ^{13}C and 2·365 MeV in ^{13}N), while level 2 represents a background due to all other $\frac{1}{2}^+$ levels.

The energy E_r of the $\frac{1}{2}^+$ level of ^{13}N is taken as the energy at which the resonant nuclear phase shift for scattering of s-wave protons on ^{12}C passes through $\frac{1}{2}\pi$. From the phase shift

$$\delta_\mathrm{p}(E) = \arctan[R_\mathrm{p} P_\mathrm{p}/\{1 - R_\mathrm{p}(S_\mathrm{p} - B_\mathrm{p})\}] - \phi_\mathrm{p}, \tag{3}$$

we therefore obtain

$$R_\mathrm{p}(E_\mathrm{r}) = 1/\{S_\mathrm{p}(E_\mathrm{r}) - B_\mathrm{p}\}. \tag{4}$$

Similarly, from the formula for the many-level density of states function (Barker 1967) applied to the $\frac{1}{2}^+$ states of ^{13}C, the energy E_b of the bound $\frac{1}{2}^+$ state of ^{13}C is given by

$$R_\mathrm{n}(E_\mathrm{b}) = 1/\{S_\mathrm{n}(E_\mathrm{b}) - B_\mathrm{n}\}. \tag{5}$$

The effective range expansion of the phase shift for scattering of s-wave neutrons on ^{12}C is

$$k \cot \delta_\mathrm{n}(E) = -a_\mathrm{s}^{-1} + \tfrac{1}{2} r_0 k^2 + \dots, \tag{6}$$

where k is the wave number ($k^2 = 2ME/\hbar^2$, with M the reduced mass). Taken together with the R-function expression for the phase shift,

$$\delta_\mathrm{n}(E) = \arctan\{kaR_\mathrm{n}/(1 + R_\mathrm{n} B_\mathrm{n})\} - ka, \tag{7}$$

this gives

$$R_\mathrm{n}(0) = \left(\frac{a}{a - a_\mathrm{s}} - B_\mathrm{n}\right)^{-1}, \tag{8}$$

$$\left(\frac{\mathrm{d}R_\mathrm{n}^{-1}(E)}{\mathrm{d}E}\right)_{E=0} = -\frac{2M}{\hbar^2}\frac{a^2 a_\mathrm{s}^2}{(a - a_\mathrm{s})^2}\left(1 - \frac{a}{a_\mathrm{s}} + \frac{a^2}{3a_\mathrm{s}^2} - \frac{r_0}{2a}\right). \tag{9}$$

The left-hand side of equation (9) is just the zero-energy value of the quantity $\{-\gamma_n^2(E)\}^{-1}$, defined in equation (IV. 2. 8) of Lane and Thomas (1958),

$$\gamma^2(E) = R^2(E)\{dR(E)/dE\}^{-1}, \tag{10}$$

which is independent of the value of B.

The observed width of the $\frac{1}{2}^+$ level of ^{13}N can be simply expressed in terms of $\gamma_p^2(E_r)$, by assuming that P_p and ϕ_p are constant over the width of the level and S_p is a linear function of E; then if the observed width Γ^o is defined as the difference in the energies at which $\delta_p(E)$ is $\frac{1}{4}\pi$ greater than or less than the resonance value, one has

$$\left(\frac{dR_p^{-1}(E)}{dE}\right)_{E=E_r} \equiv -\gamma_p^{-2}(E_r) = \frac{dS_p(E_r)}{dE} - \frac{2P_p(E_r)}{\Gamma^o}. \tag{11}$$

We note that $\gamma_p^2(E_r)$ is the value of γ_{1p}^2 corresponding to $B_p = S_p(E_r)$. With this choice of B_p, equation (11) can be written as

$$\Gamma^o = \frac{\Gamma}{1+\gamma_{1p}^2\, dS_p(E_r)/dE}, \tag{12}$$

where $\Gamma = 2\gamma_{1p}^2 P_p(E_r)$ is the formal width. It is the observed width rather than the formal width that approximates the full width at half maximum of a resonance peak, which is usually quoted as the experimental width of a level.

Restrictions on the $\frac{1}{2}^+$ level parameters are then obtained by substituting from equations (2) into equations (4), (5), (8), (9) and (11), and fitting the experimental data on the $\frac{1}{2}^+$ levels in Table 1.

In order to discuss the transition probabilities, we now consider formulae for the capture cross sections and E1 radiative widths. In their Section XIII. 3, Lane and Thomas (1958) dealt with the inclusion of photon channels in the R-matrix theory and showed that photons play a role in nuclear reactions similar to that of heavy particles. One difference is that the external region may contribute to the electromagnetic transition matrix elements. Thomas (1952) showed the importance of such contributions in the case of E1 transitions in ^{13}C and ^{13}N. Thomas used a one-channel approximation to describe the internal as well as the external region. Lane and Thomas argued that even in many-channel cases, the external transitions are significant only in channels in which there are incident waves. We also assume this, limiting external contributions to the ^{12}C ground-state channel alone, with the extension that for transitions between bound states, we also include contributions from this channel only. In cases of radiative transitions in which a one-level approximation is assumed for the initial state or the initial state is bound, we consider formulae for the radiative width, in other cases for the capture cross section.

For simplicity we first assume the one-channel approximation for both the internal and external regions. The E1 capture cross section in either ^{13}C or ^{13}N, from an initial continuum state i to a final bound state f, each with definite J^π values, can be written (Rolfs 1973)

$$\sigma_\gamma(\mathrm{i}\to\mathrm{f}) = \frac{2\pi M}{\hbar^2 k_\mathrm{i}^3}(2J_\mathrm{i}+1)f_\mathrm{if}\left|\int_0^\infty r\,u_\mathrm{i}(r)\,u_\mathrm{f}(r)\,dr\right|^2\Big/\int_0^\infty u_\mathrm{f}^2(r)\,dr, \tag{13}$$

where

$$f_\mathrm{if} = \tfrac{4}{3}(\tfrac{6}{13})^2 e^2(E_\gamma/\hbar c)^3(l_\mathrm{i}\,100\,|\,l_\mathrm{f}\,0)^2\,U^2(1\,l_\mathrm{f}\,J_\mathrm{i}\,\tfrac{1}{2};l_\mathrm{i}\,J_\mathrm{f}). \tag{14}$$

Here J_q and l_q (q = i, f) are the total and orbital angular momenta of the state q and $u_q(r)/r$ is its radial wavefunction. The long wavelength approximation for the E1 operator is assumed, and the spin part of the E1 operator is neglected (Blatt and Weisskopf 1952). The normalization of the continuum state is such that we have

$$u_{\mathrm{i}}(r) = F_{l_{\mathrm{i}}}(r)\cos\delta_{\mathrm{i}} + G_{l_{\mathrm{i}}}(r)\sin\delta_{\mathrm{i}} \qquad (r \geqslant a), \tag{15}$$

where $F_{l_{\mathrm{i}}}$ and $G_{l_{\mathrm{i}}}$ are the regular and irregular Coulomb functions and δ_{i} is the nuclear phase shift for the state i, which is given by a formula such as (3) or (7).

In order to obtain a formula for the radiative width of the transition i → f, we then use the one-level approximation (1) for the R function and equate the resulting expression for σ_γ with the one-level form of the cross section,

$$\sigma_\gamma(\mathrm{i}\to\mathrm{f}) = \frac{\pi}{k_{\mathrm{i}}^2}\frac{2J_{\mathrm{i}}+1}{2}\frac{2\gamma_{\mathrm{i}}^2 P_{\mathrm{i}}\Gamma_\gamma(\mathrm{i}\to\mathrm{f})}{\{E_{\mathrm{i}}-\gamma_{\mathrm{i}}^2(S_{\mathrm{i}}-B_{\mathrm{i}})-E\}^2+(\gamma_{\mathrm{i}}^2 P_{\mathrm{i}})^2}, \tag{16}$$

where γ_{i}^2 stands for $\gamma_{\mathrm{1n}}^2(J_{\mathrm{i}}^{\pi_{\mathrm{i}}})$ or $\gamma_{\mathrm{1p}}^2(J_{\mathrm{i}}^{\pi_{\mathrm{i}}})$ as appropriate, and P_{i} stands for $P_{\mathrm{n}}(J_{\mathrm{i}}^{\pi_{\mathrm{i}}})$ or $P_{\mathrm{p}}(J_{\mathrm{i}}^{\pi_{\mathrm{i}}})$, etc. By using the relation

$$\gamma_{\mathrm{i}}^2 = \frac{\hbar^2}{2Ma}u_{\mathrm{i}}^2(a)\Big/\int_0^a u_{\mathrm{i}}^2(r)\,\mathrm{d}r, \tag{17}$$

we obtain

$$\Gamma_\gamma(\mathrm{i}\to\mathrm{f}) = f_{\mathrm{if}}\left|\int_0^\infty r\,u_{\mathrm{i}}(r)\,u_{\mathrm{f}}(r)\,\mathrm{d}r\right|^2\Big/\left(\int_0^a u_{\mathrm{i}}^2(r)\,\mathrm{d}r\int_0^\infty u_{\mathrm{f}}^2(r)\,\mathrm{d}r\right). \tag{18}$$

This is a formula for the formal radiative width, since the shift factor S_{i} is included explicitly in equation (16). The observed radiative width is given by (cf. equation 12)

$$\Gamma_\gamma^{\mathrm{o}}(\mathrm{i}\to\mathrm{f}) = \frac{\Gamma_\gamma(\mathrm{i}\to\mathrm{f})}{1+\gamma_{\mathrm{i}}^2\,\mathrm{d}S_{\mathrm{i}}/\mathrm{d}E}. \tag{19}$$

For an E1 radiative transition between two bound states, one has (Blatt and Weisskopf 1952)

$$\Gamma_\gamma^{\mathrm{o}}(\mathrm{i}\to\mathrm{f}) = f_{\mathrm{if}}\left|\int_0^\infty r\,u_{\mathrm{i}}(r)\,u_{\mathrm{f}}(r)\,\mathrm{d}r\right|^2\Big/\left(\int_0^\infty u_{\mathrm{i}}^2(r)\,\mathrm{d}r\int_0^\infty u_{\mathrm{f}}^2(r)\,\mathrm{d}r\right), \tag{20}$$

which can be written in the form of equations (18) and (19), since

$$\int_0^\infty u^2(r)\,\mathrm{d}r = (1+\gamma^2\,\mathrm{d}S/\mathrm{d}E)\int_0^a u^2(r)\,\mathrm{d}r \tag{21}$$

for a bound state (Lane and Thomas 1958).

A formula for the cross section for E1 capture from one continuum state to another has been given by Rolfs and Azuma (1974). When one notes that the quantity Γ entering their expression (16) for the cross section is the observed width of the final state, and if one makes a one-level approximation for the initial state, one finds that the formal radiative width is of the form (18) except that $\int_0^\infty u_{\mathrm{f}}^2(r)\,\mathrm{d}r$ is replaced by $(1+\gamma_{\mathrm{f}}^2\,\mathrm{d}S_{\mathrm{f}}/\mathrm{d}E)\int_0^a u_{\mathrm{f}}^2(r)\,\mathrm{d}r$ (for a bound state f, these are identical because of equation

21). Thus an expression for the observed radiative width, valid for the states i and f being either bound or continuum states, is

$$\Gamma_{\gamma}^{o}(\mathrm{i} \to \mathrm{f}) = f_{\mathrm{if}} \left| \int_0^{\infty} r\, u_{\mathrm{i}}(r)\, u_{\mathrm{f}}(r)\, \mathrm{d}r \right|^2 \Bigg/ \left((1 + \gamma_{\mathrm{i}}^2\, \mathrm{d}S_{\mathrm{i}}/\mathrm{d}E)(1 + \gamma_{\mathrm{f}}^2\, \mathrm{d}S_{\mathrm{f}}/\mathrm{d}E) \times \int_0^a u_{\mathrm{i}}^2(r)\, \mathrm{d}r \int_0^a u_{\mathrm{f}}^2(r)\, \mathrm{d}r \right). \tag{22}$$

Some authors (Christy and Duck 1961; Tombrello and Parker 1963) have replaced $\int_0^{\infty} u_{\mathrm{f}}^2(r)\,\mathrm{d}r$ in equation (13) by $\int_0^a u_{\mathrm{f}}^2(r)\,\mathrm{d}r$, which is equivalent to omitting the factor $1 + \gamma_{\mathrm{f}}^2\, \mathrm{d}S_{\mathrm{f}}/\mathrm{d}E$ in equation (22). The normalization given in equation (13) is also used by Thomas (1952) and Lane and Thomas (1958), although we note that in his actual fitting of the data, Thomas replaced his factor N by 1, thus effectively using the normalization of Christy and Duck.

As in Thomas (1952), we separate the radial integrals occurring in equation (13) into internal and external parts, by introducing the dimensionless internal transition moment $\mathscr{M}_{\mathrm{if}}$ and other dimensionless quantities

$$\mathscr{M}_{\mathrm{if}} = a^{-1} \int_0^a r\, u_{\mathrm{i}}(r)\, u_{\mathrm{f}}(r)\, \mathrm{d}r \Bigg/ \left(\int_0^a u_{\mathrm{i}}^2(r)\, \mathrm{d}r \int_0^a u_{\mathrm{f}}^2(r)\, \mathrm{d}r \right)^{\frac{1}{2}}, \tag{23a}$$

$$\Theta_q = u_q(a) \left(\tfrac{1}{2} a \Bigg/ \int_0^a u_q^2(r)\, \mathrm{d}r \right)^{\frac{1}{2}}, \tag{23b}$$

$$J_{\mathrm{if}} = a^{-2} \int_a^{\infty} r\, w_{\mathrm{i}}(r)\, w_{\mathrm{f}}(r)\, \mathrm{d}r, \qquad w_q(r) = u_q(r)/u_q(a), \tag{23c}$$

$$N_q = 1 + \gamma_q^2\, \mathrm{d}S_q/\mathrm{d}E. \tag{23d}$$

Then, by making use of equation (21), equation (13) can be written

$$\sigma_{\gamma}(\mathrm{i} \to \mathrm{f}) = \frac{2\pi M}{\hbar^2 k_{\mathrm{i}}^3} (2J_{\mathrm{i}} + 1) f_{\mathrm{if}} \frac{a^3 u_{\mathrm{i}}^2(a)}{2N_{\mathrm{f}}\, \Theta_{\mathrm{i}}^2} | \mathscr{M}_{\mathrm{if}} + 2\Theta_{\mathrm{i}}\, \Theta_{\mathrm{f}}\, J_{\mathrm{if}} |^2. \tag{24}$$

The additional factor of 2 in the external contribution in equation (24) relative to Thomas's formula (40c) is due to the additional factor of $\frac{1}{2}$ in the definition of Θ_q in equation (23b). This is introduced in order to retain the usual relationship between the Θ_q and the reduced width amplitude γ_q (Lane and Thomas 1958),

$$\gamma_q = (\hbar^2/Ma^2)^{\frac{1}{2}} \Theta_q. \tag{25}$$

In a similar way, equation (22) can be written

$$\Gamma_{\gamma}^{o}(\mathrm{i} \to \mathrm{f}) = f_{\mathrm{if}} (a^2/N_{\mathrm{i}}\, N_{\mathrm{f}}) | \mathscr{M}_{\mathrm{if}} + 2\Theta_{\mathrm{i}}\, \Theta_{\mathrm{f}}\, J_{\mathrm{if}} |^2. \tag{26}$$

Now we drop the assumption that the internal region can be described in the one-channel approximation. Since we still assume that the external contributions come from the ^{12}C ground-state channel alone, the form of equations (24) and (26) is unchanged, but the definitions (23a, b) of $\mathscr{M}_{\mathrm{if}}$ and Θ_q are changed. Shell model formulae for $\mathscr{M}_{\mathrm{if}}$ and Θ_q are given in Section 5.

In fitting the experimental data on capture cross sections and radiative widths by means of equations (24) and (26), we treat the quantities $\mathscr{M}_{\rm if}$ and Θ_q as parameters, the other quantities being calculable in terms of the known asymptotic forms of the radial wavefunctions. Among the latter quantities are the radial integrals $J_{\rm if}$. The $u_q(r)$ for $r \geqslant a$, which occur in $J_{\rm if}$, are either bound-state wavefunctions, determined by the binding energy of the state, or continuum wavefunctions given by equation (15) in terms of the nuclear phase shift δ_q. This phase shift is required only for $J^\pi = \frac{1}{2}^+$ or $\frac{3}{2}^-$ (see Fig. 1); for the $\frac{3}{2}^-$ case δ_q is needed only on resonance, where it has the value $\frac{1}{2}\pi - \phi_q$, while for the $\frac{1}{2}^+$ case δ_q is given by equation (3) or (7) in terms of the level parameters of the $\frac{1}{2}^+$ levels. The integration in $J_{\rm if}$ can be performed analytically for the ^{13}C cases and numerically for the ^{13}N cases. For the $\frac{3}{2}^- \to \frac{1}{2}^+$ transition in ^{13}N, there is the problem that both the states i and f belong to the continuum, so that the integral cannot be evaluated in a straightforward manner. Faessler (1965) and Rolfs and Azuma (1974) have shown how the Ehrenfest theorem can be used to evaluate the integral* in such a case when the limits of integration are 0 and ∞. The same method can be used for the integration from a to ∞, except that additional contributions come from the lower limit. It is still assumed that the integrated parts vanish at ∞. We find

$$\begin{aligned}\int_a^\infty r\,u_{\rm i}(r)\,u_{\rm f}(r)\,{\rm d}r = \frac{\hbar^2}{ME_\gamma^2}\bigg\{&\int_a^\infty V^{\rm C\prime}(r)\,u_{\rm i}(r)\,u_{\rm f}(r)\,{\rm d}r - \frac{\hbar^2}{2M}u_{\rm i}'(a)\,u_{\rm f}'(a)\\ &+\tfrac{1}{2}a\Big(E_\gamma + \{l_{\rm i}(l_{\rm i}+1) - l_{\rm f}(l_{\rm f}+1)\}\frac{\hbar^2}{2Ma^2}\Big)\{u_{\rm i}'(a)\,u_{\rm f}(a) - u_{\rm i}(a)\,u_{\rm f}'(a)\}\\ &-\tfrac{1}{2}\Big(E({\rm i}) + E({\rm f}) - 2V^{\rm C}(a) - \{l_{\rm i}(l_{\rm i}+1) + l_{\rm f}(l_{\rm f}+1)\}\frac{\hbar^2}{2Ma^2}\Big)u_{\rm i}(a)\,u_{\rm f}(a)\bigg\}, \qquad (27)\end{aligned}$$

where $V^{\rm C}(r)$ is the Coulomb potential, $E(q)$ is the energy of the state q and $E_\gamma = E({\rm i}) - E({\rm f})$. The right-hand side of equation (27) depends only on $u_q(r)$ for $r \geqslant a$. Since $V^{\rm C\prime}(r) \propto r^{-2}$, the integral on the right-hand side can be evaluated numerically.

4. Fits to Data

The R-matrix formulae of Section 3 are now used to fit the experimental data of Table 1 in order to derive values of the parameters E_λ, $\gamma_{\lambda c}$ (or γ_q) and $\mathscr{M}_{\rm if}$. Written more fully, these are $E_{\lambda{\rm n}}(J^\pi)$ or $E_{\lambda{\rm p}}(J^\pi)$, $\gamma_{\lambda{\rm n}}(J^\pi)$ or $\gamma_{\lambda{\rm p}}(J^\pi)$ and $\mathscr{M}(J_{\rm i}^{\pi_{\rm i}} \to J_{\rm f}^{\pi_{\rm f}})$. We assume that the $\mathscr{M}_{\rm if}$ depend only on $J_{\rm i}^{\pi_{\rm i}}$ and $J_{\rm f}^{\pi_{\rm f}}$, and do not depend on the particular energies of the states i and f or on whether the transition is in ^{13}C or ^{13}N. Then for ^{13}C, we note that $\mathscr{M}(\frac{3}{2}^- \to \frac{1}{2}^+) = \mathscr{M}(\frac{1}{2}^+ \to \frac{3}{2}^-)$. In some cases we consider Θ_q rather than γ_q, since these are related by equation (25).

For the $\frac{1}{2}^+$ levels of ^{13}C and ^{13}N there are five pieces of data given in Table 1, but the formulae (2) for the R functions contain eight unknowns. We therefore reduce the number of background parameters, which we cannot expect to be well determined by the data, by assuming that $E_{2{\rm p}} - E_{1{\rm p}} = E_{2{\rm n}} - E_{1{\rm n}}$ and $\gamma_{2{\rm p}}^2 = \gamma_{2{\rm n}}^2$, provided that, say, $B_{\rm p} = B_{\rm n} = B$ (this makes the quality of fit dependent on the choice

* This method works only for the integral $\int r\,u_{\rm i}(r)\,u_{\rm f}(r)\,{\rm d}r$, which is obtained *after* the long wavelength approximation has been assumed, and justification of this approximation is difficult for an integral that is not convergent.

of B, since $\gamma^2_{1p} \neq \gamma^2_{1n}$, but this dependence is not significant for reasonable values of B). We also take $E_{2n} = 10$ MeV; varying this value does not change significantly any of the results, except the value of γ^2_{2n}. Thus for given values of a and B, the remaining five adjustable parameters E_{1n}, E_{1p}, γ^2_{1n}, γ^2_{1p} and γ^2_{2n} can be determined. Values of γ^2_{1n} for $B = S_n(E_b)$ and of γ^2_{1p} for $B = S_p(E_r)$ are shown in Fig. 2a as functions of a. As a decreases, values of γ^2_{2n} decrease and become negative for $a < 4{\cdot}2$ fm so that the solutions are inadmissible; for $a \approx 4{\cdot}2$ fm, a one-level approximation for the $\frac{1}{2}^+$ levels therefore gives an acceptable fit to the data.

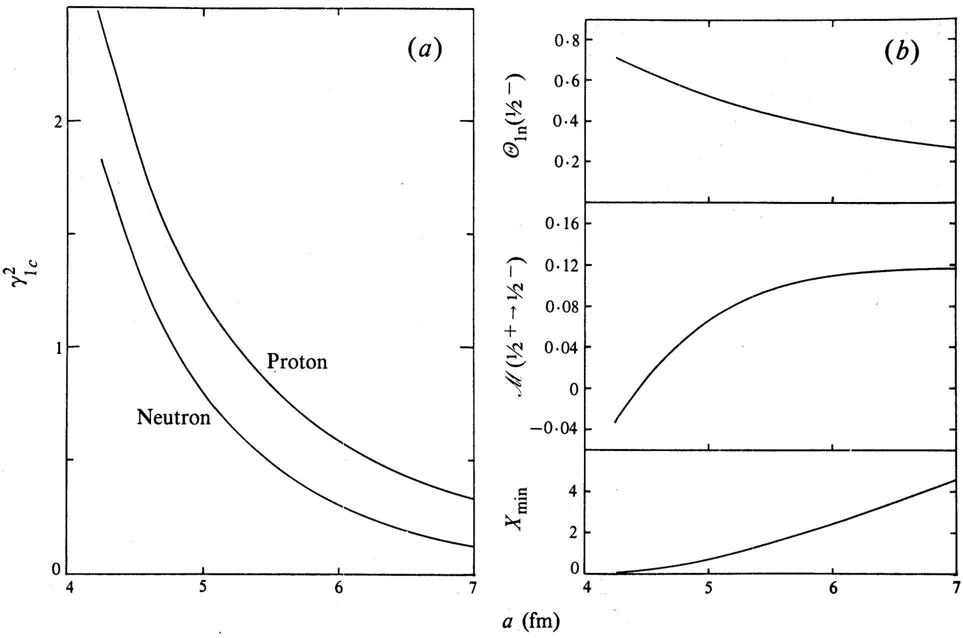

Fig. 2. Values of parameters as functions of the channel radius a: (a) the reduced widths γ^2_{1n} and γ^2_{1p} for the $\frac{1}{2}^+$ levels obtained by fitting the data in Table 1 and (b) $\Theta_{1n}(\frac{1}{2}^-)$, $\mathscr{M}(\frac{1}{2}^+ \to \frac{1}{2}^-)$ and X_{min} obtained by a least squares fit of the data in Table 1.

The formulae (24) and (26) for the E1 capture cross sections and radiative widths involve level parameters for the $\frac{1}{2}^-$, $\frac{1}{2}^+$, $\frac{3}{2}^-$ and $\frac{5}{2}^+$ levels and internal transition moments $\mathscr{M}_{if}$. Values of the $\frac{1}{2}^+$ level parameters are known from the above fits. Thus in formula (24), which is required only for $\frac{1}{2}^+ \to \frac{1}{2}^-$ transitions, the value of Θ_i is obtained from equations (25), (10) and (2), while $u_i(a)$ is obtained from equation (15) with δ_i given by (3) or (7) together with (2). For the levels with $J^\pi \neq \frac{1}{2}^+$ the level energies are known, so one is left with the adjustable parameters $\gamma_q \equiv \gamma_{\lambda c}$ (or $\Theta_{\lambda c}$) for these levels and the $\mathscr{M}_{if}$. Because of the scarcity of data we take Θ_{1n} and Θ_{1p} as being related but not necessarily equal. We use the shell model expression for the $\Theta_{\lambda c}$ (equation 32 in Section 5) and assume $\mathscr{S}^{\frac{1}{2}}_{1n} = \mathscr{S}^{\frac{1}{2}}_{1p}$, but allow $u_{1n}(r)$ and $u_{1p}(r)$ to be different by taking them as Woods–Saxon wavefunctions with appropriate boundary conditions. Thus, Θ_{1p} is expressed as a multiple of Θ_{1n}, and only Θ_{1n} and $\mathscr{M}_{if}$ are adjusted. They are chosen to minimize the quantity

$$X = \frac{1}{N-2} \sum_{i=1}^{N} \left| \frac{V_{calc}(i) - V_{exp}(i)}{\varepsilon(i)} \right|^2, \qquad (28)$$

where $V_{calc}(i)$, $V_{exp}(i)$ and $\varepsilon(i)$ are the calculated and experimental values and the error of the quantity i, and N data are fitted.

For the five pieces of data in Table 1 involving transitions between the $\frac{1}{2}^+$ and $\frac{1}{2}^-$ levels, the best fit values of $\Theta_{1n}(\frac{1}{2}^-)$, $\mathscr{M}(\frac{1}{2}^+ \rightarrow \frac{1}{2}^-)$ and X_{min} are shown in Fig. 2*b* as functions of a. It is seen that the best fits occur for the smaller values of a, those for $a \lesssim 6$ fm being regarded as acceptable. Values for $a = 5$ fm are given in the last column of Table 1, and in Table 2. Reasonable changes in the data in Table 1 involving the $\frac{1}{2}^+$ levels and the $\frac{1}{2}^+ \rightarrow \frac{1}{2}^-$ transitions have little effect on either the values of the parameters or the quality of fit, except that smaller values of X_{min} are obtained if $\Gamma_\gamma^o(^{13}C, \frac{1}{2}^+ \rightarrow \frac{1}{2}^-)$ is increased or $\sigma_{p\gamma}(E_r)$ is decreased.

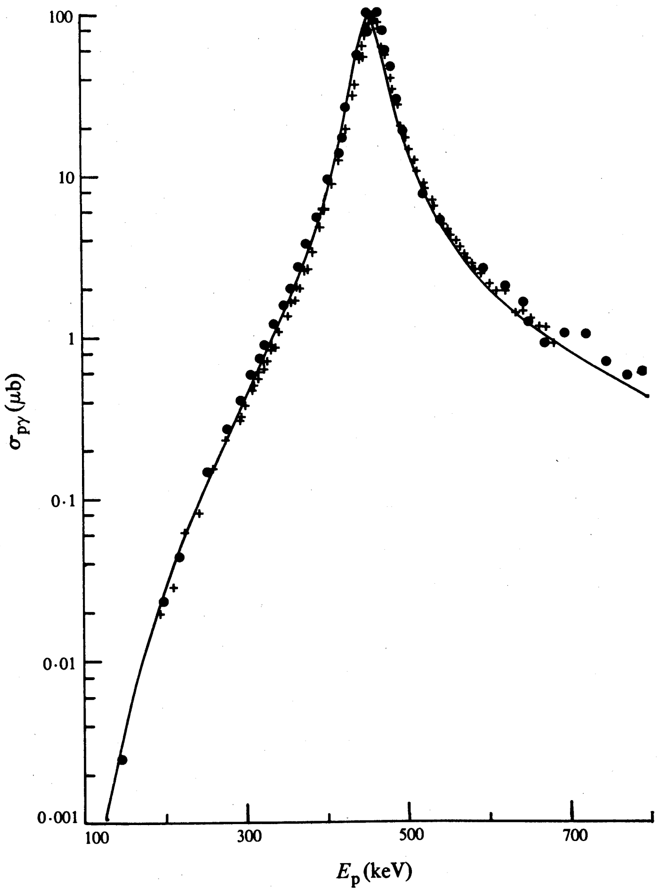

Fig. 3. The $^{12}C(p, \gamma_0)^{13}N$ cross section $\sigma_{p\gamma}$ as a function of proton energy E_p. The curve gives the calculated values for a channel radius $a = 5$ fm. Experimental points (plusses, Vogl 1963; circles, Rolfs and Azuma 1974) are renormalized to a peak cross section of 102 μb.

The values of $\Theta_{1n}(\frac{1}{2}^-)$ and $\mathscr{M}(\frac{1}{2}^+ \rightarrow \frac{1}{2}^-)$ in Fig. 2*b* do not agree with the values Thomas (1952) obtained, which correspond to region I of his Fig. 6, but do agree with his alternative solution in region II (see Barker 1961). Thomas's preference for region I was based mainly on his study of the displacements of corresponding levels in ^{13}C and ^{13}N (see Section 6). It is our inclusion of the radiative width of the $\frac{1}{2}^+$ state of ^{13}C in the fit that excludes parameter values corresponding to region I.

Among the fitted data are the ^{12}C(p, γ_0)^{13}N cross section at three energies ($E_p = 120$ 456 and 604 keV). From the parameter values we can calculate the cross section at other energies. Fig. 3 shows the calculated cross section for $a = 5$ fm, together with the renormalized experimental points of Vogl (1963) and Rolfs and Azuma (1974). (The Rolfs and Azuma values were deduced from the S factors given in Fig. 5 of Rolfs and Azuma and Fig. 4 of Fox *et al.* (1975), since accurate values could not be obtained from the 0° and 90° excitation functions plotted by Rolfs and Azuma.) The agreement seems to be reasonable.

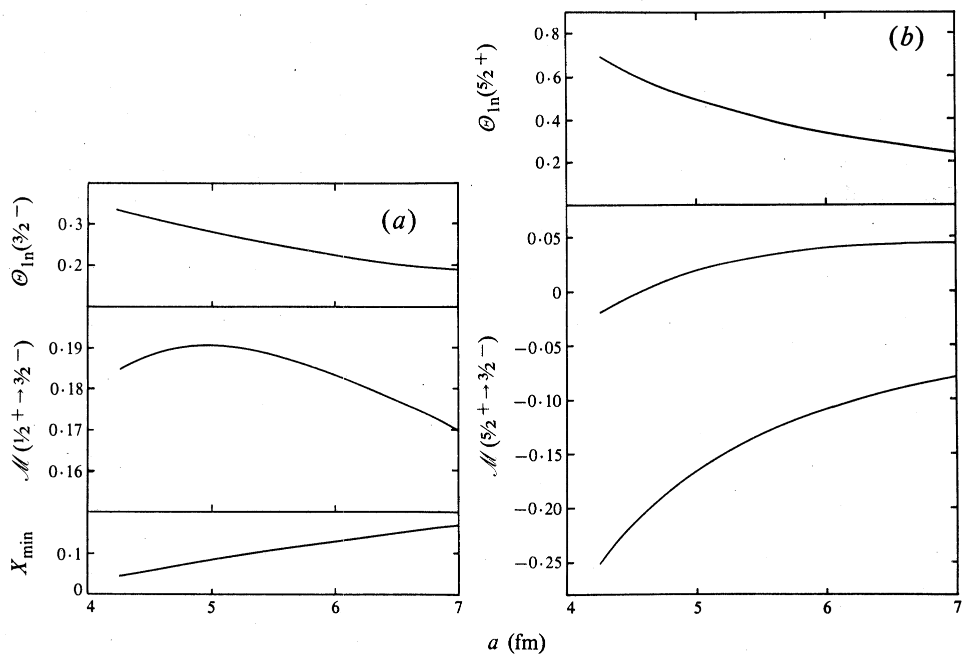

Fig. 4. Values of parameters as functions of the channel radius a: (*a*) $\Theta_{1n}(\frac{3}{2}^-)$, $\mathscr{M}(\frac{1}{2}^+ \to \frac{3}{2}^-)$ and X_{min} obtained by a least squares fit of the data in Table 1 and (*b*) $\Theta_{1n}(\frac{5}{2}^+)$ and $\mathscr{M}(\frac{5}{2}^+ \to \frac{3}{2}^-)$ obtained by fitting the data in Table 1.

The S factor for the ^{12}C(p, γ_0)^{13}N reaction at low energies is required in astrophysical calculations. The value at $E_{c.m.} = 25$ keV has been given as $S = 1\cdot33 \pm 0\cdot15$ keV b (Hebbard and Vogl 1960) and $1\cdot45 \pm 0\cdot20$ keV b (Rolfs and Azuma 1974). Since their normalization of the peak cross section was different from ours, we might expect a different value of S. Our best fit for $a = 5$ fm gives $S = 1\cdot54$ keV b, with estimated uncertainties of $\pm 0\cdot08$ keV b due to experimental errors and $^{+0\cdot07}_{-0\cdot02}$ keV b due to an uncertainty of $\pm 1\cdot0$ fm in the value of a. Thus our S value is somewhat higher than the earlier values.

Similar fits are made to the three pieces of data in Table 1 involving transitions between the $\frac{1}{2}^+$ and $\frac{3}{2}^-$ levels. The observed width of the $\frac{3}{2}^-$ level of ^{13}N is not fitted at this stage, since its calculated value is expected to depend appreciably on the contribution to the level shift from the ^{12}C first-excited state channel, and this involves a further unknown parameter. The best fit values of $\Theta_{1n}(\frac{3}{2}^-)$, $\mathscr{M}(\frac{1}{2}^+ \to \frac{3}{2}^-)$ and $X_{\min}$ are shown in Fig. 4*a*. Again the best fits occur for the smaller values of *a*. Values for $a = 5$ fm are given in Tables 1 and 2. Changes in the $\frac{1}{2}^+$ data or the $\frac{3}{2}^- \leftrightarrow \frac{1}{2}^+$ transition data by the uncertainties given in Table 1 have little effect on the values of the parameters and the quality of fit remains acceptable. The effect of larger changes in some of the data is discussed in Section 7.

The remaining data in Table 1 involve the $\frac{5}{2}^+$ level and its decay to the $\frac{3}{2}^-$ level. It is reasonable to assume a one-level, one-channel approximation to fit the observed width of the $\frac{5}{2}^+$ level of ^{13}N, and this gives $\Theta_{1p}(\frac{5}{2}^+)$ as a function of *a*. From this one obtains values of $\Theta_{1n}(\frac{5}{2}^+)$, and from the previous fits one has $\Theta_{1n}(\frac{3}{2}^-)$, so that the measured value of $\Gamma_\gamma^0(^{13}\mathrm{C}, \frac{5}{2}^+ \to \frac{3}{2}^-)$ can be fitted by adjusting the remaining parameter $\mathscr{M}(\frac{5}{2}^+ \to \frac{3}{2}^-)$. Fig. 4*b* shows the values of $\Theta_{1n}(\frac{5}{2}^+)$ and the two solutions for $\mathscr{M}(\frac{5}{2}^+ \to \frac{3}{2}^-)$ as functions of *a*.

5. Level Parameters from Shell Model Calculations and Other Experimental Data

Figs 2 and 4 contain values of the reduced widths γ_{1n}^2 and γ_{1p}^2 for the $\frac{1}{2}^+$ levels, dimensionless reduced width amplitudes Θ_{1n} for the $\frac{1}{2}^-$, $\frac{3}{2}^-$ and $\frac{5}{2}^+$ levels, and internal transition moments $\mathscr{M}(\frac{1}{2}^+ \to \frac{1}{2}^-)$, $\mathscr{M}(\frac{1}{2}^+ \to \frac{3}{2}^-)$ and $\mathscr{M}(\frac{5}{2}^+ \to \frac{3}{2}^-)$, obtained by fitting experimental data. Calculated values of each of these quantities may be obtained from shell model descriptions of the states, and values of $\Theta_{\lambda c}$ are also available from single-nucleon transfer reactions, which have not been discussed so far.

For the negative (normal) parity $A = 13$ states, we use the *LS* coupling representation in the lowest $(1s^4\,1p^9)$ configuration,

$$\Psi_{13}(TM_T J^-) = \sum_{[\lambda]SL} a([\lambda]TSLJ)\,\Psi(1s^4\,1p^9[\lambda]TSLM_T J)\,, \tag{29}$$

where $T = \frac{1}{2}$, $M_T = +\frac{1}{2}, -\frac{1}{2}$ for ^{13}C, ^{13}N respectively, $J = \frac{1}{2}$ or $\frac{3}{2}$, and $[\lambda]$ is the orbital symmetry. For describing the channels consisting of an $A = 12$ nucleus plus a nucleon, we need the $A = 12$ wavefunctions, which we take to be normal-parity states of the lowest configuration,

$$\Psi_{12}(\bar{T}\bar{M}_T\bar{J}) = \sum_{[\bar{\lambda}]\bar{S}\bar{L}} \bar{a}([\bar{\lambda}]\bar{T}\bar{S}\bar{L}\,\bar{J})\,\Psi(1s^4\,1p^8[\bar{\lambda}]\bar{T}\bar{S}\bar{L}\bar{M}_T\bar{J})\,. \tag{30}$$

For the present purpose, this description is required only for the ^{12}C ground and first excited states ($\bar{T} = \bar{M}_T = 0$, $\bar{J} = 0$ or 2), but a more general formalism is needed for use in Section 6.

The positive (non-normal) parity $A = 13$ states are written (Barker 1961)

$$\Psi_{13}(TM_T J^+) = \sum_{\bar{J}j} b(T\bar{J}jJ)\,\Psi\big((\bar{J}j)TM_T J\big)\,, \tag{31}$$

where T and M_T are as before and $J = \frac{1}{2}$ or $\frac{5}{2}$. The $\bar{J}$ in Ψ represents the core states $\Psi_{12}(00\bar{J})$ of equation (30) with $\bar{J} = 0$ or 2 only, and j is an abbreviation for *nlj*, with $nl = 2$s or 1d. We omit other basis states that are included in some of the more elaborate shell model calculations for the $A = 13$ positive-parity states (e.g. Jäger *et al.* 1971).

Formulae for calculating the reduced width amplitude for a level λ and a channel c are given by Lane (1960). These are of the form

$$\Theta_{\lambda c} = \mathscr{S}^{\frac{1}{2}}_{\lambda c}\, u_c(a)\left(\tfrac{1}{2}a\Big/\int_0^a u_c^2(r)\,\mathrm{d}r\right)^{\frac{1}{2}}, \tag{32}$$

which replaces the one-channel formula (23b). The $\mathscr{S}^{\frac{1}{2}}_{\lambda c}$ are spectroscopic amplitudes. For the negative-parity $A = 13$ states, these are given by

$$\begin{aligned}\mathscr{S}^{\frac{1}{2}}_{\lambda c} &\equiv \mathscr{S}^{\frac{1}{2}}(J^- M_T, \bar{J}\bar{T}\bar{M}_T j)\\ &= \sum_{[\lambda]SL[\bar{\lambda}]\bar{S}\bar{L}} a([\lambda]\tfrac{1}{2}SLJ)\,\bar{a}([\bar{\lambda}]\bar{T}\bar{S}\bar{L}\bar{J})\,\mathscr{S}^{\frac{1}{2}}([\lambda]\tfrac{1}{2}SLM_T J, [\bar{\lambda}]\bar{T}\bar{S}\bar{L}\bar{M}_T\bar{J}j),\end{aligned} \tag{33}$$

where

$$\begin{aligned}&\mathscr{S}^{\frac{1}{2}}([\lambda]TSLM_T J, [\bar{\lambda}]\bar{T}\bar{S}\bar{L}\bar{M}_T\bar{J}j)\\ &\quad= 3(\bar{T}\tfrac{1}{2}\bar{M}_T M_T - \bar{M}_T \mid TM_T)\langle 1\mathrm{p}^9[\lambda]TSL\{\mid 1\mathrm{p}^8[\bar{\lambda}]\bar{T}\bar{S}\bar{L}, 1\mathrm{p}\rangle\\ &\qquad\times\{(2\bar{J}+1)(2j+1)(2S+1)(2L+1)\}^{\frac{1}{2}}\begin{Bmatrix}\bar{S} & \bar{L} & \bar{J}\\ \frac{1}{2} & 1 & j\\ S & L & J\end{Bmatrix},\end{aligned} \tag{34}$$

involving a Clebsch–Gordan coefficient, a fractional parentage coefficient and a $9j$ symbol. The label j is here the angular momentum of the odd 1p nucleon. At present $\mathscr{S}^{\frac{1}{2}}_{\lambda c}$ is required only for the ^{12}C ground-state channel, for which $j = J$. For the positive-parity $A = 13$ states

$$\mathscr{S}^{\frac{1}{2}}(J^+ M_T, \bar{J}\bar{T}\bar{M}_T j) = b(\tfrac{1}{2}\bar{J}jJ)\,\delta(\bar{T},0)\,\delta(\bar{M}_T,0). \tag{35}$$

The $u_c(r)$ in equation (32) are taken as wavefunctions in a Woods–Saxon potential with the conventional parameter values $r_0 = 1\cdot25$ fm and $a = 0\cdot65$ fm, and a uniform charge distribution with radius $1\cdot25$ fm, the depth in each case being chosen to fit the observed separation energy for a wavefunction with the correct l value and the appropriate number of nodes.

Comparison between experiment and calculation is made in the values of $\mathscr{S}^{\frac{1}{2}}_{\lambda c}$, in particular for the level labelled $\lambda = 1$ and for the ^{12}C ground-state channel labelled $c = \mathrm{g}$. The experimental values of $\mathscr{S}^{\frac{1}{2}}_{1\mathrm{g}}$ for the various J^π values are obtained by making use of equations (25) and (32), and the calculated values are obtained from equations (33)–(35). In each case we assume $\mathscr{S}^{\frac{1}{2}}_{1\mathrm{g}} > 0$ and $u_{\mathrm{g}}(a) > 0$, which is consistent with the positive values of $\Theta_{\lambda c}$ assumed in Section 4; it also implies a certain sign convention for the shell model states, which must be retained in calculating values of $\mathscr{M}_{\mathrm{if}}$. For the negative-parity levels, shell model values of $\mathscr{S}_{1\mathrm{g}}$ are given by Cohen and Kurath (1967) and by Varma and Goldhammer (1969). For the positive-parity levels, we give only two sets of values; those of Barker (1961) represent weak-coupling calculations, while those of Jäger *et al.* (1971) are from complete calculations within the space of all $1\hbar\omega$ excitations. These values are given in Table 3. Other calculated values are not essentially different from these. The curves in Fig. 5 show the experimental values of $\mathscr{S}^{\frac{1}{2}}_{1\mathrm{g}}$ plotted as functions of a, while the calculated values, which are independent of a, are indicated on the left. There is reasonable agreement between the calculated and experimental values. For the $\frac{1}{2}^+$ case, the experimental value of $\mathscr{S}^{\frac{1}{2}}_{1\mathrm{g}}$ obtained from the best ^{13}N (proton) data is somewhat different from that from the ^{13}C (neutron) data, but equal values can be achieved for $a \lesssim 6$ fm when allowance is made for the experimental uncertainties in r_0 and $\Gamma^\mathrm{o}(^{13}\mathrm{N}, \frac{1}{2}^+)$.

Table 3. Spectroscopic factors of ^{13}C and ^{13}N low-lying levels for ^{12}C ground-state channels

$\mathscr{S}_{1\mathrm{g}}$ $\frac{1}{2}^-$	$\frac{1}{2}^+$	$\frac{3}{2}^-$	$\frac{5}{2}^+$	Reaction	Ref.[A]
Calculated					
0·61		0·19			a
0·56		0·10			b
	0·97		0·81		c
	0·89		0·81		d
Experimental					
0·8	0·9	0·26	0·8	^{12}C(d, p)^{13}C	e
1·16		0·22		^{12}C(d, p)^{13}C	f
0·58±0·15	0·36±0·02			^{12}C(d, p)^{13}C	g
1·1, 1·4	1·1, 1·2	0·10, 0·20	1·1, 1·4	^{12}C(d, p)^{13}C	h
0·53±0·12				^{12}C(d, n)^{13}N	g
0·82				^{13}C(p, d)^{12}C	i
0·7–1·48	0·25	~0·02	~0·14	^{12}C(^{3}He, d)^{13}N	j
0·68				^{12}C(^{3}He, d)^{13}N	k
0·52				^{13}C(d, t)^{12}C	l
0·80	0·44	0·17	0·74	^{12}C(^{7}Li, ^{6}Li)^{13}C	m
0·72				^{12}C(^{7}Li, ^{6}He)^{13}N	m
0·25, 0·40	0·38, 0·61		0·23, 0·37	^{12}C(^{10}B, ^{9}Be)^{13}N	n
0·66				^{12}C(^{13}C, ^{12}C)^{13}C	o
0·81				^{12}C(^{13}C, ^{12}C)^{13}C	p
0·59±0·12				^{12}C(^{13}C, ^{12}C)^{13}C	q
0·81±0·04				^{12}C(^{13}C, ^{13}C)^{12}C	r
0·72			0·57	^{12}C(^{14}N, ^{13}N)^{13}C	s
0·62	0·09		0·49	^{12}C(^{14}N, ^{13}C)^{13}N	s

[A] References: a, Cohen and Kurath (1965); b, Varma and Goldhammer (1969); c, Barker (1961); d, Jäger *et al.* (1971); e, Glover and Jones (1966); f, Schiffer *et al.* (1967); g, Pearson *et al.* (1972); h, Darden *et al.* (1973); i, Taketani *et al.* (1968); j, Fortune *et al.* (1969); k, Karban *et al.* (1976); l, Ludwig *et al.* (1974); m, Zeller *et al.* (1979); n, Nair *et al.* (1974); o, DeVries (1973); p, Von Oertzen and Bohlen (1975); q, Bennett (1976); r, Gubler *et al.* (1977); s, Nair *et al.* (1975).

In Section 4, the observed width of the $\frac{3}{2}^-$ second excited state of ^{13}N was not fitted, due to the expected importance of ^{12}C excited-state channels. In the one-level, many-channel approximation, the observed width is given by

$$\Gamma^\mathrm{o} = 2\gamma_{1\mathrm{g}}^2 P_\mathrm{g} \Big/ \left(1 + \sum_c \gamma_{1c}^2 \mathrm{d}S_c/\mathrm{d}E\right), \tag{36}$$

where the subscript $c = \mathrm{g}$ again indicates the ^{12}C ground-state channel, which is the only one open, and the sum over c includes all open and closed channels. For $c \neq \mathrm{g}$, we use values of γ_{1c}^2 obtained from calculated values of $\mathscr{S}_{1c}$ (for the POT interaction of Cohen and Kurath 1965). Then the value of $\gamma_{1\mathrm{g}}^2$ in equation (36) is adjusted for each value of a in order to fit the measured value $\Gamma^\mathrm{o}(^{13}\mathrm{N}, \frac{3}{2}^-) = 60 \pm 5$ keV (see Table 1). Table 4 gives the shell model values of $\mathscr{S}_{1c}$ for the more important excited-state channels, and the corresponding values of $\gamma_{1c}^2\, \mathrm{d}S_c/\mathrm{d}E$ for a few values of a. The resultant values of $\mathscr{S}_{1g}^{\frac{1}{2}} \equiv \{\mathscr{S}_{1g}(\frac{3}{2}^-)\}^{\frac{1}{2}}$ are shown as a function of a by the dashed curve in Fig. 5, the uncertainty being of the order of 5% due to the experimental error in Γ°. There is good agreement between the value of $\mathscr{S}_{1g}^{\frac{1}{2}}$ obtained in this way and that obtained in Section 4.

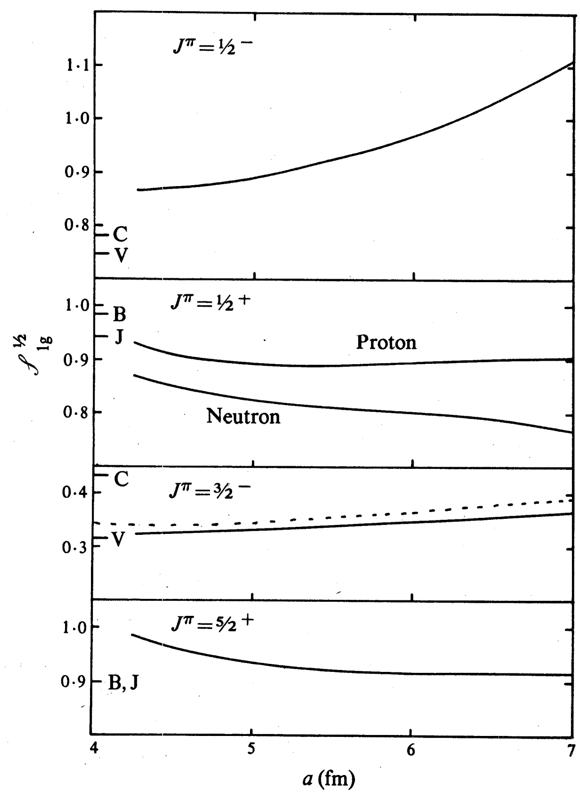

Fig. 5. Values of the spectroscopic amplitudes $\mathscr{S}_{1g}^{\frac{1}{2}}$ as functions of channel radius a, for levels with the J^{π} values indicated and for the ^{12}C ground-state channel. Solid curves are experimental values derived from the fits shown in Figs 2 and 4. The dashed curve is obtained by fitting $\Gamma^{\circ}(^{13}\mathrm{N}, \frac{3}{2}^-)$ using equation (36). Calculated shell model values are indicated along the ordinate with labels C (Cohen and Kurath 1967), V (Varma and Goldhammer 1969), B (Barker 1961) and J (Jäger *et al.* 1971).

Analyses of single-nucleon transfer reactions by DWBA or an equivalent formalism also provide values of the $\mathscr{S}_{1g}$. Some of these values are collected in Table 3. It is seen that they vary widely, particularly for the excited ^{13}C and ^{13}N states, and in general their agreement with the theoretical values is much poorer than that indicated in Fig. 5. It is interesting to note that the recent work of Franey *et al.* (1979) on the ^{12}C(^{17}O,^{16}O)^{13}C reaction, although it does not quote a value of $\mathscr{S}_{1g}(\frac{1}{2}^-)$ as such, obtains results in excellent agreement with the ^{12}C(^{13}C,^{13}C)^{12}C study by Gubler *et al.* (1977), whose value of $\mathscr{S}_{1g}(\frac{1}{2}^-)$ in Table 3 is in good agreement with the experimental values in Fig. 5.

Table 4. Calculated quantities entering equation (36) for the observed width of the ^{13}N $\frac{3}{2}^-$ state

Channel c E_x (MeV)	JT	$\mathscr{S}_{1c}$	$\gamma_{1c}^2\,\mathrm{d}S_c/\mathrm{d}E$ $a = 4$ fm	$a = 5$ fm	$a = 6$ fm
4·44	20	1·143	0·250	0·093	0·036
12·71	10	0·206	0·015	0·003	0·001
15·11	11	0·803	0·046	0·009	0·001
16·11	21	0·120	0·006	0·001	0·000

Now we require a shell model formula for $\mathscr{M}_{\mathrm{if}}$, which appears in equations (24) and (26). The radiative width for an E1 transition from a positive-parity bound state i given by equation (31) to a negative-parity bound state f given by equation (29) is (Blatt and Weisskopf 1952)

$$\Gamma_\gamma^0(\mathrm{i}\to\mathrm{f}) = \frac{16\pi}{9}\left(\frac{E_\gamma}{\hbar c}\right)^3 |\langle J_\mathrm{i}\,\|\,Q_1\,\|\,J_\mathrm{f}\rangle|^2\,, \tag{37}$$

where

$$Q_{1\mu,\mathrm{op}} = \tfrac{1}{2}e\sum_{i=1}^{A}\left(\frac{N-Z}{A}-\tau_3(i)\right)r(i)\,Y_{1\mu}(\Omega_i)\,. \tag{38}$$

Substituting from equations (29) and (31), and making use of formulae (33)–(35), we obtain

$$\begin{aligned}\langle J_\mathrm{i}\,\|\,Q_1\,\|\,J_\mathrm{f}\rangle = {}& e\left(\frac{3}{4\pi}\right)^{\frac{1}{2}}\tfrac{12}{13}M_T\sum_{\bar{J}j_\mathrm{i}j_\mathrm{f}}(l_\mathrm{i}\,100\,|\,10)\,U(11j_\mathrm{i}\tfrac{1}{2};l_\mathrm{i}j_\mathrm{f})\\ &\times U(1j_\mathrm{f}J_\mathrm{i}\bar{J};j_\mathrm{i}J_\mathrm{f})\,\mathscr{S}^{\frac{1}{2}}(J_\mathrm{i}^+,\bar{J}j_\mathrm{i})\,\mathscr{S}^{\frac{1}{2}}(J_\mathrm{f}^-,\bar{J}j_\mathrm{f})\\ &\times\int_0^\infty r\,u_{\bar{J}j_\mathrm{i}}(r)\,u_{\bar{J}j_\mathrm{f}}(r)\,\mathrm{d}r\bigg/\left(\int_0^\infty u_{\bar{J}j_\mathrm{i}}^2(r)\,\mathrm{d}r\int_0^\infty u_{\bar{J}j_\mathrm{f}}^2(r)\,\mathrm{d}r\right)^{\frac{1}{2}},\end{aligned} \tag{39}$$

where $\mathscr{S}^{\frac{1}{2}}(J^\pi M_T,\bar{J}00j)$ has been written $\mathscr{S}^{\frac{1}{2}}(J^\pi,\bar{J}j)$. With Θ_q given by equation (32) we find that equation (37) is of the form (26) provided that

$$\begin{aligned}\mathscr{M}_{\mathrm{if}} = {}& \frac{1}{(l_\mathrm{g}\,100\,|\,10)\,U(11J_\mathrm{i}\tfrac{1}{2};l_\mathrm{g}J_\mathrm{f})}\\ &\times\left(\int_0^\infty u_{0J_\mathrm{i}}^2(r)\,\mathrm{d}r\int_0^\infty u_{0J_\mathrm{f}}^2(r)\,\mathrm{d}r\bigg/\int_0^a u_{0J_\mathrm{i}}^2(r)\,\mathrm{d}r\int_0^a u_{0J_\mathrm{f}}^2(r)\,\mathrm{d}r\right)^{\frac{1}{2}}\\ &\times\sum_{\bar{J}j_\mathrm{i}j_\mathrm{f}}(l_\mathrm{i}\,100\,|\,10)\,U(11j_\mathrm{i}\tfrac{1}{2};l_\mathrm{i}j_\mathrm{f})\,U(1j_\mathrm{f}J_\mathrm{i}\bar{J};j_\mathrm{i}J_\mathrm{f})\,\mathscr{S}^{\frac{1}{2}}(J_\mathrm{i}^+,\bar{J}j_\mathrm{i})\,\mathscr{S}^{\frac{1}{2}}(J_\mathrm{f}^-,\bar{J}j_\mathrm{f})\\ &\times a^{-1}\int_0^a r\,u_{\bar{J}j_\mathrm{i}}(r)\,u_{\bar{J}j_\mathrm{f}}(r)\,\mathrm{d}r\bigg/\left(\int_0^\infty u_{\bar{J}j_\mathrm{i}}^2(r)\,\mathrm{d}r\int_0^\infty u_{\bar{J}j_\mathrm{f}}^2(r)\,\mathrm{d}r\right)^{\frac{1}{2}}.\end{aligned} \tag{40}$$

Then equation (40) is the shell model generalization of the one-channel formula (23a).

In evaluating $\mathscr{M}_{\mathrm{if}}$ from equation (40), we make the approximations that the $u_{\bar{J}j}(r)$ are harmonic oscillator single-particle wavefunctions $u_{nl}(r)$, and that the upper limits of the integrals in equation (40) can be extended from a to ∞ (cf. similar approximations in Barker 1978), and assume that the same formula can be applied to transitions involving continuum states. Then

$$\mathscr{M}_{\mathrm{if}} = \frac{1}{(l_{\mathrm{g}}\,100\,|\,10)\,U(11J_{\mathrm{i}}\tfrac{1}{2};l_{\mathrm{g}}J_{\mathrm{f}})}\sum_{\bar{J}j_{\mathrm{i}}j_{\mathrm{f}}}(l_{\mathrm{i}}\,100\,|\,10)\,U(11j_{\mathrm{i}}\tfrac{1}{2};l_{\mathrm{i}}j_{\mathrm{f}})$$
$$\times U(1j_{\mathrm{f}}J_{\mathrm{i}}\bar{J};j_{\mathrm{i}}J_{\mathrm{f}})\,\mathscr{S}^{\frac{1}{2}}(J_{\mathrm{i}}^{+},\bar{J}j_{\mathrm{i}})\,\mathscr{S}^{\frac{1}{2}}(J_{\mathrm{f}}^{-},\bar{J}j_{\mathrm{f}})\,a^{-1}I_{n_{\mathrm{i}}l_{\mathrm{i}}}, \tag{41}$$

where

$$I_{2\mathrm{s}} = b, \qquad I_{1\mathrm{d}} = (\tfrac{5}{2})^{\frac{1}{2}}b, \tag{42}$$

and b is the harmonic oscillator length parameter.* Thus

$$\mathscr{M}(\tfrac{1}{2}^{+}\to\tfrac{1}{2}^{-}) = ba^{-1}[\mathscr{S}^{\frac{1}{2}}(\tfrac{1}{2}^{+},0\tfrac{1}{2})\,\mathscr{S}^{\frac{1}{2}}(\tfrac{1}{2}^{-},0\tfrac{1}{2})$$
$$+\{-\surd\tfrac{1}{10}\mathscr{S}^{\frac{1}{2}}(\tfrac{1}{2}^{+},2\tfrac{3}{2})+6\surd\tfrac{1}{15}\mathscr{S}^{\frac{1}{2}}(\tfrac{1}{2}^{+},2\tfrac{5}{2})\}\,\mathscr{S}^{\frac{1}{2}}(\tfrac{1}{2}^{-},2\tfrac{3}{2})], \tag{43a}$$

$$\mathscr{M}(\tfrac{1}{2}^{+}\to\tfrac{3}{2}^{-}) = ba^{-1}[\mathscr{S}^{\frac{1}{2}}(\tfrac{1}{2}^{+},0\tfrac{1}{2})\,\mathscr{S}^{\frac{1}{2}}(\tfrac{3}{2}^{-},0\tfrac{3}{2})-\tfrac{1}{2}\surd5\,\mathscr{S}^{\frac{1}{2}}(\tfrac{1}{2}^{+},2\tfrac{3}{2})\,\mathscr{S}^{\frac{1}{2}}(\tfrac{3}{2}^{-},2\tfrac{1}{2})$$
$$-\surd\tfrac{1}{5}\mathscr{S}^{\frac{1}{2}}(\tfrac{1}{2}^{+},2\tfrac{3}{2})\,\mathscr{S}^{\frac{1}{2}}(\tfrac{3}{2}^{-},2\tfrac{3}{2})-3\surd\tfrac{1}{30}\mathscr{S}^{\frac{1}{2}}(\tfrac{1}{2}^{+},2\tfrac{5}{2})\,\mathscr{S}^{\frac{1}{2}}(\tfrac{3}{2}^{-},2\tfrac{3}{2})], \tag{43b}$$

$$\mathscr{M}(\tfrac{5}{2}^{+}\to\tfrac{3}{2}^{-}) = ba^{-1}[\tfrac{1}{2}\surd10\,\mathscr{S}^{\frac{1}{2}}(\tfrac{5}{2}^{+},0\tfrac{5}{2})\,\mathscr{S}^{\frac{1}{2}}(\tfrac{3}{2}^{-},0\tfrac{3}{2})-\tfrac{2}{3}\mathscr{S}^{\frac{1}{2}}(\tfrac{5}{2}^{+},2\tfrac{1}{2})\,\mathscr{S}^{\frac{1}{2}}(\tfrac{3}{2}^{-},2\tfrac{1}{2})$$
$$-\tfrac{1}{3}\mathscr{S}^{\frac{1}{2}}(\tfrac{5}{2}^{+},2\tfrac{1}{2})\,\mathscr{S}^{\frac{1}{2}}(\tfrac{3}{2}^{-},2\tfrac{3}{2})+\tfrac{1}{6}\surd35\,\mathscr{S}^{\frac{1}{2}}(\tfrac{5}{2}^{+},2\tfrac{3}{2})\,\mathscr{S}^{\frac{1}{2}}(\tfrac{3}{2}^{-},2\tfrac{1}{2})$$
$$-\tfrac{1}{15}\surd35\,\mathscr{S}^{\frac{1}{2}}(\tfrac{5}{2}^{+},2\tfrac{3}{2})\,\mathscr{S}^{\frac{1}{2}}(\tfrac{3}{2}^{-},2\tfrac{3}{2})+\tfrac{1}{5}\surd35\,\mathscr{S}^{\frac{1}{2}}(\tfrac{5}{2}^{+},2\tfrac{5}{2})\,\mathscr{S}^{\frac{1}{2}}(\tfrac{3}{2}^{-},2\tfrac{3}{2})]. \tag{43c}$$

Table 5. Shell model values of spectroscopic amplitudes $\mathscr{S}^{\frac{1}{2}}(J^{\pi}, \bar{J}j)$

J^{π}	$\bar{J}=$ 0, $j=\frac{1}{2}$	0, $\frac{3}{2}$	0, $\frac{5}{2}$	2, $\frac{1}{2}$	2, $\frac{3}{2}$	2, $\frac{5}{2}$
$\frac{1}{2}^{-}$	0·783				−1·059	
$\frac{3}{2}^{-}$		0·433		0·910	0·561	
$\frac{1}{2}^{+}$	0·943				0·120	0·270
$\frac{5}{2}^{+}$			0·899	0·149	−0·095	−0·373

Values of $\mathscr{S}^{\frac{1}{2}}(J^{-},\bar{J}j)$ for the POT interaction of Cohen and Kurath (1965) and of $\mathscr{S}^{\frac{1}{2}}(J^{+},\bar{J}j)$ from Jäger *et al.* (1971) are given in Table 5. With these values, the coefficients of b/a in the expressions (43) for $\mathscr{M}(\frac{1}{2}^{+}\to\frac{1}{2}^{-})$, $\mathscr{M}(\frac{1}{2}^{+}\to\frac{3}{2}^{-})$ and $\mathscr{M}(\frac{5}{2}^{+}\to\frac{3}{2}^{-})$ are 0·336, 0·173 and 0·186 respectively. With $b = 1\cdot67$ fm from elastic electron scattering on ^{12}C (Ajzenberg-Selove 1976), these values of $\mathscr{M}$ are plotted as dashed curves in Fig. 6 as functions of a, while the solid curves give the best fit values from Section 4.

* For consistency with our convention that $u_c(a) > 0$ for the ^{12}C ground-state channel, we have to choose the sign of $u_{2s}(r)$ opposite to that in Barker (1961); otherwise, our sign conventions are the same regarding the order of coupling of angular momenta.

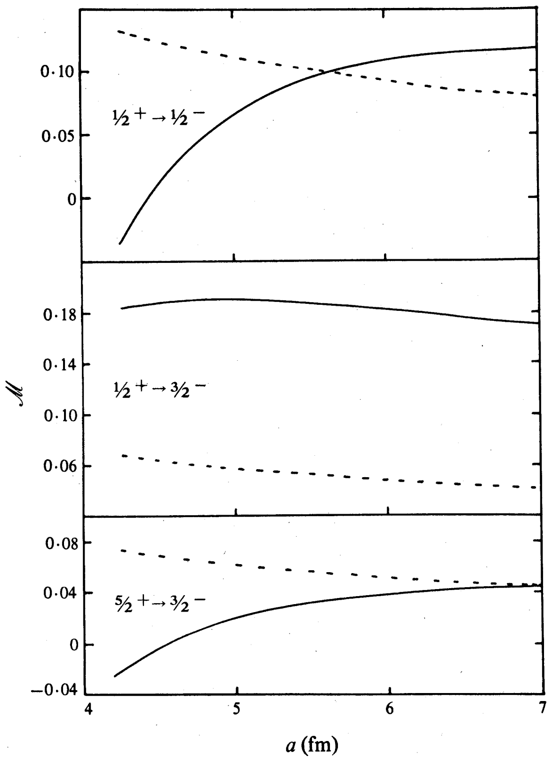

Fig. 6. Values of E1 internal transition moments $\mathscr{M}$ as functions of the channel radius a, for the transitions indicated. Solid curves are experimental values derived from the fits shown in Figs 2 and 4, using the upper solution in the $\frac{5}{2}^+ \rightarrow \frac{3}{2}^-$ case since this gives better agreement. Dashed curves give the calculated shell model values.

It is seen that there is agreement between calculated and experimental values of $\mathscr{M}(\frac{1}{2}^+ \rightarrow \frac{1}{2}^-)$ for $a \approx 5\cdot5$ fm, but this particular value is probably not very significant. The calculated values are very sensitive to the values of $\mathscr{S}^{\frac{1}{2}}(\frac{1}{2}^+, \bar{J}j)$; for example, they are increased by a factor of 1·6 if these $\mathscr{S}$ values are taken from Barker (1961), and by a factor of 2·3 if the one-channel approximation is used for the $\frac{1}{2}^+$ level $\big(\mathscr{S}^{\frac{1}{2}}(\frac{1}{2}^+, 0\frac{1}{2}) = 1\big)$. Thus agreement could be obtained for smaller values of a, which are favoured from the fits in Section 4, if $\mathscr{S}^{\frac{1}{2}}(\frac{1}{2}^+, 0\frac{1}{2})$ were somewhat smaller than the value of Jäger *et al.* (1971). Additional support for this comes from Fig. 5.

The calculated and experimental values of $\mathscr{M}(\frac{1}{2}^+ \rightarrow \frac{3}{2}^-)$ are quite different. The small calculated value is due to cancellation between the term having the ^{12}C ground state as parent and those having the ^{12}C excited state as parent, being only about 40% of the value in the one-channel approximation. Even this, however, is less than the experimental value, and agreement would require ^{12}C ground- and excited-state contributions of the same sign. This discrepancy is discussed further in Section 7. Similarly, the calculated values of $\mathscr{M}(\frac{5}{2}^+ \rightarrow \frac{3}{2}^-)$ are sensitive to $\mathscr{S}^{\frac{1}{2}}(\frac{5}{2}^+, \bar{J}j)$, the value for the $\mathscr{S}$ values of Jäger *et al.* being only 27% of that obtained with $\mathscr{S}^{\frac{1}{2}}(\frac{5}{2}^+, 0\frac{5}{2}) = 1$.

6. Coulomb Displacement Energies

In Fig. 1, the level energies of ^{13}C and ^{13}N are adjusted to make the ground-state energies the same. The actual binding-energy difference between analogue states of the same J^{π}, known as the Coulomb displacement energy, is defined by

$$\Delta E_C(J^{\pi}) = M(^{13}\mathrm{N}, J^{\pi}) - M(^{13}\mathrm{C}, J^{\pi}) + \delta_{\mathrm{np}}, \tag{44}$$

where δ_{np} is the neutron–proton mass difference and all masses are atomic masses. The experimental values of ΔE_C for the $\frac{1}{2}^-$, $\frac{1}{2}^+$, $\frac{3}{2}^-$ and $\frac{5}{2}^+$ states shown in Fig. 1 are 3003, 2280, 2830 and 2696 keV respectively (Ajzenberg-Selove 1976).

Thomas (1952) attempted to fit the *net displacements* of these levels, i.e. the differences of the Coulomb displacement energy for each pair of excited states from that for the ground states. These are the energy differences apparent in Fig. 1. Thomas considered three contributions to the net displacements, resulting from the internal Coulomb interaction, the electromagnetic spin–orbit interaction and the different external wavefunctions in ^{13}C and ^{13}N. The last contribution he also called the boundary-condition level displacement. The internal Coulomb energies were not calculated but were estimated to vary by not more than ± 200 keV in the different states. The other two contributions were calculated assuming that each state could be represented as a single nucleon outside an inert ^{12}C ground-state core. The depression of the $\frac{1}{2}^+$ state in ^{13}N relative to that in ^{13}C was attributed mainly to the boundary-condition contribution, i.e. the Thomas–Ehrman effect.

Coulomb displacement energies have been studied in other mirror systems, and many different contributions to them have been considered. In a recent review article, Shlomo (1978) lists and discusses these contributions, in particular for systems with one particle or one hole outside closed shells. He finds that, in first-order perturbation theory, the inclusion of various correction terms (see Table 6 of Shlomo 1978) does not remove the discrepancy between calculated and experimental Coulomb displacement energies that exists for the point Coulomb interaction alone; this is the Okamoto–Nolen–Schiffer anomaly. Shlomo considers also higher order perturbation effects, such as isospin mixing in the core, and suggests that the discrepancy of about 7% still remaining may, for the lighter mirror nuclei, be attributed largely to charge-symmetry-breaking nuclear potentials.

We now calculate the Coulomb displacement energies for the ^{13}N–^{13}C pairs of levels, including the point Coulomb contribution and the various correction terms of Shlomo (1978) in first-order perturbation theory, but omitting higher order perturbation effects and charge-symmetry-breaking nuclear potentials. Thus we should not expect to obtain quantitative agreement with the experimental values. Because we use shell model wavefunctions (Cohen and Kurath 1965; Jäger *et al.* 1971), the calculation of some contributions is more complicated than in the cases considered by Shlomo. In particular, the boundary-condition contribution, which Shlomo obtained by taking the difference of matrix elements of the Coulomb interaction calculated with harmonic oscillator and Woods–Saxon potentials, is calculated here using the Bloch operator (Bloch 1957; Lane and Robson 1966). Following the procedure and notation of Barker (1978), we write for each J^{π} value

$$H\Psi_{M_T} = E_{M_T}\Psi_{M_T}, \tag{45a}$$

with

$$\mathscr{L}(S_{M_T})\Psi_{M_T} = 0, \tag{45b}$$

where H is the total Hamiltonian, $\mathscr{L}(S)$ the Bloch operator and $M_T = +\frac{1}{2}, -\frac{1}{2}$ for ^{13}C, ^{13}N respectively. The eigenfunctions Ψ_{M_T} are expanded in terms of states $\Psi_{Tn}(M_T)$ of good isospin T,

$$\Psi_{M_T} = \sum_{Tn} A_{M_T}^{Tn} \Psi_{Tn}(M_T), \tag{46}$$

which satisfy

$$H^0 \Psi_{Tn}(M_T) = E_{Tn}^0 \Psi_{Tn}(M_T), \qquad \mathscr{L}(\bar{S}_{Tn}) \Psi_{Tn}(M_T) = 0, \tag{47a, b}$$

where

$$H = H^0 + H^c, \tag{48}$$

and H^0 is the charge-independent part of the Hamiltonian. The E_{Tn}^0 and $\bar{S}_{Tn}$ are independent of M_T, so that the dependence of $\Psi_{Tn}(M_T)$ on M_T is trivial, whereas the dependence of Ψ_{M_T} on M_T is all important. Then to first order in the charge-dependent effects (H^c and $S_{M_T} - \bar{S}_{Tn}$), one has

$$E_{M_T} = E_{\frac{1}{2}1}^0 + \langle \Psi_{\frac{1}{2}1}(M_T) | H^c + \mathscr{L}(S_{M_T}) - \mathscr{L}(\bar{S}_{\frac{1}{2}1}) | \Psi_{\frac{1}{2}1}(M_T) \rangle . \tag{49}$$

Then the Coulomb displacement energy is given by

$$\Delta E_C \equiv E_{-\frac{1}{2}} - E_{\frac{1}{2}} = \Delta H^c + \Delta L, \tag{50}$$

where

$$\Delta H^c = \langle \Psi_{\frac{1}{2}1}(-\tfrac{1}{2}) | H^c | \Psi_{\frac{1}{2}1}(-\tfrac{1}{2}) \rangle - \langle \Psi_{\frac{1}{2}1}(\tfrac{1}{2}) | H^c | \Psi_{\frac{1}{2}1}(\tfrac{1}{2}) \rangle , \tag{51a}$$

$$\Delta L = \langle \Psi_{\frac{1}{2}1}(-\tfrac{1}{2}) | \mathscr{L}(S_{-\frac{1}{2}}) - \mathscr{L}(\bar{S}_{\frac{1}{2}1}) | \Psi_{\frac{1}{2}1}(-\tfrac{1}{2}) \rangle - \langle \Psi_{\frac{1}{2}1}(\tfrac{1}{2}) | \mathscr{L}(S_{\frac{1}{2}}) - \mathscr{L}(\bar{S}_{\frac{1}{2}1}) | \Psi_{\frac{1}{2}1}(\tfrac{1}{2}) \rangle . \tag{51b}$$

We include contributions to ΔL from the nucleon channels $c \equiv \tilde{c}m_t$, for which

$$(c | \Psi_{\frac{1}{2}1}(M_T) \rangle = u_{\tilde{c}}(r_c) \mathscr{S}_{\tilde{c}}^{\frac{1}{2}} (\tilde{T} \tfrac{1}{2} M_T - m_t m_t | \tfrac{1}{2} M_T), \tag{52}$$

so that

$$\Delta L = -\sum_c \frac{\hbar^2}{2m_{\tilde{c}} a_{\tilde{c}}} u_{\tilde{c}}^2(a_c) \mathscr{S}_{\tilde{c}} \sum_{m_t} \{ (\tilde{T} \tfrac{1}{2} - \tfrac{1}{2} - m_t m_t | \tfrac{1}{2} - \tfrac{1}{2})^2 S_{-\frac{1}{2}}(\tilde{c}m_t)$$
$$- (\tilde{T} \tfrac{1}{2} \tfrac{1}{2} - m_t m_t | \tfrac{1}{2} \tfrac{1}{2})^2 S_{\frac{1}{2}}(\tilde{c}m_t) \} . \tag{53}$$

Terms in ΔL containing $\bar{S}_{\frac{1}{2}1}$ vanish. We include contributions to ΔL from the channels involving $A = 12$ levels identified as belonging to the lowest shell model configuration (Cohen and Kurath 1965), i.e. the lowest 0^+, 2^+ and 1^+ $T = 0$ states of ^{12}C at 0·0, 4·44 and 12·71 MeV, and the lowest two $T = 1$ states (1^+ and 2^+) of the ^{12}B, ^{12}C and ^{12}N triad (at 15·11 and 16·11 MeV in ^{12}C). The separate contributions to ΔL are listed in Table 6 for a particular choice of channel radius $a_c = 5$ fm. The dependence on a_c is discussed later.

Contributions to ΔH^c are calculated for the point Coulomb interaction and the correction terms discussed by Shlomo (1978). Matrix elements of the Coulomb interaction are calculated with harmonic oscillator radial wavefunctions as discussed by Barker (1978), using standard shell model techniques, as are those of the magnetic interactions. Other contributions are evaluated as in Shlomo (1978). The results are given in Table 6. The shell model wavefunctions are those of Cohen and Kurath (1965) with the POT interaction for the negative-parity states and those of Jäger *et al.* (1971) for the positive-parity states (including only the ^{12}C 0^+ and 2^+ $T = 0$ states as core states). The harmonic oscillator parameter is taken as $b = 1 \cdot 67$ fm, as before.

Table 6. Contributions (in keV) to Coulomb displacement energies for ^{13}C and ^{13}N levels

Contribution $J^\pi =$	$\frac{1}{2}^-$		$\frac{1}{2}^+$		$\frac{3}{2}^-$		$\frac{5}{2}^+$	
Point Coulomb		2916		2828		2929		2707
Boundary condition ($a_c = 5$ fm)								
channel $0^+, T = 0$	−80		−623		−111		−201	
$2^+, T = 0$	−52		−3		−105		−14	
$1^+, T = 0$	−8		0		−4		0	
$1^+, T = 1$	4		0		4		0	
$2^+, T = 1$	6		0		1		0	
Total		−130		−626		−215		−215
Centre-of-mass motion		−84		−67		−82		−75
Finite size of proton		107		88		104		95
Finite size of neutron		−49		−50		−50		−45
Magnetic interactions								
orbit–orbit	4·5		18·8		3·9		4·6	
spin–orbit	42		−6		56		−63	
tensor	1·5		0		0·5		0	
$\rho_p(r)$ term	0·3		3·2		0·8		4·3	
Total		48		16		61		−54
Vacuum polarization		17		13		16		15
p–n mass difference		26		36		26		36
Short-range correlation		59		24		52		30
Total (calc.)		2910		2262		2841		2494
Experimental		3003		2280		2830		2696
Discrepancy		93		18		−11		202

Some comments may be made on the values in Table 6 in relation to the calculations of Thomas (1952). Although Thomas did not consider many of the terms that give large contributions to the Coulomb displacement energies, he did include those that contribute most to the net displacements. He included the boundary-condition contribution only for the ^{12}C ground-state channels, obtaining values close to those in Table 6 except for the $\frac{1}{2}^-$ states. For these, in order to obtain a better fit to the net displacement for the $\frac{3}{2}^-$ levels, he preferred a solution with a small reduced width of the $\frac{1}{2}^-$ states (corresponding to his region I) rather than the solution with larger reduced width (region II), and so obtained a contribution of only -27 keV. Such a small reduced width is, however, in conflict with more recent experimental and calculated values (see Section 4 and Fig. 5). The spin–orbit contributions in Table 6 agree reasonably with the values obtained by Thomas, except for the $\frac{3}{2}^-$ states for which his value was -20 keV. This disagreement indicates the deficiency of Thomas's model for the $\frac{3}{2}^-$ states of a $p_{3/2}$ nucleon outside a spin-zero core.

The discrepancies between the calculated and experimental values of the Coulomb displacement energies, which are shown at the bottom of Table 6, appear to be less systematic than the 3–9% deviation obtained by Shlomo (1978) for other mirror systems (see his Table 6). In part this could be the result of the sensitive dependence of our calculated values on the choice of channel radius (due to the dependence of the boundary-condition contributions). If the channel radius is changed from 5 to 4·5 fm, the discrepancies in Table 6 are changed to 167, 166, 66 and 267 keV respectively, which are 2–11% of the total values. The sensitive dependence of ΔE_C on channel radius in our calculation is not apparent in Shlomo's calculation where the boundary-condition contribution is calculated in a different way. If we use our approach for the $A = 17$ cases considered by Shlomo with his simple wavefunctions, then we get agreement with his boundary-condition contributions of about -100 and -570 keV for the $\frac{5}{2}^+$ and $\frac{1}{2}^+$ levels, for channel radii of 5·2 and 4·6 fm respectively. (Note that these are not values of Shlomo's Coulomb perturbation effect, which he refers to as the Thomas–Ehrman effect.)

Thus it seems that for reasonable values of the channel radius, the discrepancies between calculated and experimental values of the Coulomb displacement energies for these pairs of levels in ^{13}C and ^{13}N are not inconsistent with those found by Shlomo in other light nuclei, and presumably they can likewise be attributed to a part of the charge-symmetry-breaking nuclear potential.

7. Discussion

The properties of the low-lying levels of ^{13}C and ^{13}N that have aroused most interest in the past are the marked difference in excitation energies of the $\frac{1}{2}^+$ first excited states (Fig. 1) and the very different strengths of the E1 transitions from these $\frac{1}{2}^+$ states to the $\frac{1}{2}^-$ ground states (Table 2). These differences would not exist if there were exact charge symmetry of all nuclear forces.

We have attempted to fit these and other properties of the $\frac{1}{2}^+$ and $\frac{1}{2}^-$ levels in a consistent R-matrix description with a two-level approximation for the $\frac{1}{2}^+$ levels and a one-level approximation for the $\frac{1}{2}^-$ levels, and to relate the resultant level parameters with those obtained from shell model calculations. Departures from charge symmetry were obtained by including effects of the Coulomb and other electromagnetic interactions and of binding energy differences. An exact fit to the $\frac{1}{2}^+$ excitation energy difference was not sought, since we did not include the effects of a charge-symmetry-breaking nuclear potential, which is believed to contribute to Coulomb displacement energies in other cases of light mirror nuclei (Shlomo 1978); nevertheless, the main part of the energy difference appears to be attributable to the boundary-condition contribution (Thomas–Ehrman effect), as found previously (Thomas 1952).

A least squares fit of all the properties involving the $\frac{1}{2}^+$ and $\frac{1}{2}^-$ levels gives a good account of the different E1 strengths of the $\frac{1}{2}^+ \to \frac{1}{2}^-$ transitions (Table 2), with level parameters agreeing reasonably with shell model values (Figs 5 and 6). In previous discussions of the different E1 strengths, it was initially suggested (Robinson *et al.* 1968; Warburton and Weneser 1969) that the asymmetry was due to differences in the external radial wavefunctions for the $\frac{1}{2}^+$ states, which are indicated by the large Thomas–Ehrman shift. However Marrs *et al.* (1975), using a simple one-body model for the $\frac{1}{2}^+$ and $\frac{1}{2}^-$ states, with Woods–Saxon wells generating the radial wavefunctions, found no difference in the strengths of the two transitions. They concluded that simple binding energy effects of this kind could not explain the large asymmetry, and that charge-dependent configuration mixing was required. Kurath (1975) took up this suggestion and assumed that the expansion coefficients in the description (31) of the $\frac{1}{2}^+$ states were different for ^{13}C and ^{13}N, the difference being due to their different binding energies. Kurath, however, used inconsistent definitions of B(E1) in deriving his calculated and experimental values. The experimental values he quotes are in units of fm^2. For consistency the factor e^2 in his equation (2) should then be replaced by $(6/13)^2$. Fitting the experimental values then requires $\alpha_s = 0\cdot 99$, $\alpha_d = 0\cdot 15$ for ^{13}C and $\alpha_s = 0\cdot 99$, $\alpha_d = -0\cdot 11$ for ^{13}N, and Kurath's argument does not explain the difference in sign of the α_d values. This difficulty can be overcome by extending the weak-coupling model for the $\frac{1}{2}^+$ state by the inclusion of a third component, a $d_{5/2}$ nucleon coupled to the lowest 2^+ $T = 1$ state (D. Kurath, personal communication). Fox *et al.* (1975) used a coupled-channels approach, but this work is still unpublished. In the present treatment, the source of the different strengths is best discussed in terms of equation (26), applied to the $\frac{1}{2}^+ \rightarrow \frac{1}{2}^-$ transitions in ^{13}C and ^{13}N. The factor $f_{\rm if}$ gives no difference in the strengths, which are obtained by dividing $\Gamma^{\rm o}_\gamma$ by E^3_γ. The internal transition moment $\mathscr{M}_{\rm if}$ is assumed to be the same for each transition, and also the factors $N_{\rm f}$ and $\Theta_{\rm f}$ for the $\frac{1}{2}^-$ state and $\Theta_{\rm i}$ for the $\frac{1}{2}^+$ state are approximately the same. The difference comes from the factors $N_{\rm i}$ (for the $\frac{1}{2}^+$ state) and $J_{\rm if}$. For example, for $a = 5$ fm, one has $N_{\rm i}(^{13}{\rm N})/N_{\rm i}(^{13}{\rm C}) = 0\cdot 66$ and $J_{\rm if}(^{13}{\rm N})/J_{\rm if}(^{13}{\rm C}) = 2\cdot 25$. In order to fit the observed asymmetry, one then needs the internal contributions to be small compared with the channel contributions. This is expected from the shell model calculations of Cohen and Kurath (1965) and Jäger *et al.* (1971), which predict a small value of $\mathscr{M}_{\rm if}$ due to the terms involving the ^{12}C excited state as parent, largely cancelling the term involving the ^{12}C ground state (see equation 43a).

In similar fits to properties involving also the $\frac{3}{2}^-$ and $\frac{5}{2}^+$ low-lying levels, the experimental data can be satisfactorily fitted (Table 1 and Fig. 4*a*), but the resultant level parameters do not all agree with shell model values (Figs 5 and 6). We note particularly the $\frac{3}{2}^- \rightarrow \frac{1}{2}^+$ E1 transitions, which experimentally have about equal strengths in ^{13}C and ^{13}N (Table 2). The calculations do not automatically suggest equal strengths, since $N_{\rm f}(^{13}{\rm N})/N_{\rm f}(^{13}{\rm C}) = 0\cdot 66$ and $J_{\rm if}(^{13}{\rm N})/J_{\rm if}(^{13}{\rm C}) = 1\cdot 69$. Equal strengths then require a relatively large value of $\mathscr{M}_{\rm if}$, which disagrees with the shell model value (Fig. 6). Better agreement would be obtained if earlier experimental values of branching ratios were used rather than those assumed in Section 2, i.e. for the ^{13}C transition $0\cdot 65 \pm 0\cdot 1\%$ (Kane *et al.* 1960) rather than $1\cdot 6 \pm 0\cdot 3\%$ (Tryti *et al.* 1975), and for ^{13}N $5 \pm 1\%$ (Woodbury *et al.* 1954) rather than $8 \pm 1\%$ (Rolfs and Azuma 1974). These would require a smaller experimental value of $\mathscr{M}(\frac{1}{2}^+ \rightarrow \frac{3}{2}^-)$. Agreement with the other quantity involving the $\frac{3}{2}^-$ and $\frac{1}{2}^+$ levels, $\sigma_{\rm n\gamma}$(thermal), could then be retained by slight adjustment in the value of $\Theta_{\rm 1n}(\frac{3}{2}^-)$, since the channel contribution dominates the internal contribution in this case. The experimental value of $\Theta_{\rm 1n}(\frac{3}{2}^-)$ agrees better with the shell model value of Varma and Goldhammer (1969) than with that of Cohen and Kurath (1967) (see Fig. 5), suggesting that the former gives a better description of the $\frac{3}{2}^-$ state, which might lead to a better value of $\mathscr{M}(\frac{1}{2}^+ \rightarrow \frac{3}{2}^-)$. We have, however, been unable to reproduce the results of Varma and Goldhammer using the interaction of Goldhammer *et al.* (1968). Alternatively, the discrepancies in the $\mathscr{M}(\frac{1}{2}^+ \rightarrow \frac{3}{2}^-)$ and $\Theta_{\rm 1n}(\frac{3}{2}^-)$ values may be due to approximations made in our calculations, such as the use of Ehrenfest's theorem in evaluating the external contribution to this ^{13}N transition, or the assumption that external contributions come only from the ^{12}C ground-state channel; the latter is particularly significant for transitions involving the $\frac{3}{2}^-$ levels since their reduced width for the ^{12}C ground-state channel is much less than for the ^{12}C first-excited state channel (see Tables 3 and 4).

In summary, acceptable R-matrix fits have been obtained to observed properties of the low-lying levels of ^{13}C and ^{13}N, including the different excitation energies of the $\frac{1}{2}^+$ states and their different E1 decay strengths. The resultant parameter values agree reasonably with shell model predictions, except for quantities involving the $\frac{3}{2}^-$ levels.

Acknowledgment

Thanks are due to Dr S. S. Ahmad for assistance in a preliminary investigation of this problem.

Note added in proof

In using equation (27) to calculate $\Gamma_\gamma^0(\mathrm{i}\to\mathrm{f})$ for the $\frac{3}{2}^- \to \frac{1}{2}^+$ transition in ^{13}N, we took $u_q(r)$ from equation (15). Holt *et al.* (1978) have shown that, for this purpose, $u_q(r)$ should rather have the form of outgoing waves,

$$u_q(r) \propto G_{l_q}(r) + \mathrm{i}\, F_{l_q}(r) \qquad (r \gtrsim a,\ q = \mathrm{i}, \mathrm{f}),$$

since only the resonant part of the channel contribution to $\sigma_\gamma(\mathrm{i}\to\mathrm{f})$ should be included when comparison is made with the one-level approximation in order to extract a formula for the radiative width. Consequently, the fits to the $\frac{3}{2}^- \to \frac{1}{2}^+$ data are changed from those shown in Fig. 4*a*; the quality of fit is much poorer, with $X_{\min} \approx 2$ for $a \lesssim 5$ fm, although the values of $\Theta_{1\mathrm{n}}(\frac{3}{2}^-)$ and $\mathscr{M}(\frac{1}{2}^+ \to \frac{3}{2}^-)$ are reduced only slightly. In these fits a ^{13}C $\frac{3}{2}^- \to \frac{1}{2}^+$ branching ratio of $1\cdot6 \pm 0\cdot3\%$ (Tryti *et al.* 1975) has been used. A recent measurement of the branching ratio (Warburton *et al.* 1980) gives $0\cdot75 \pm 0\cdot04\%$, in agreement with the early value of $0\cdot65 \pm 0\cdot1\%$ (Kane *et al.* 1960). Use of this new value leads to much better fits, with $X_{\min} \lesssim 0\cdot2$ for $a \lesssim 6$ fm. Values given in Table 2 for the $\frac{3}{2}^- \to \frac{1}{2}^+$ transitions are changed, with the ratios becoming $2\cdot47 \pm 0\cdot68$ (experiment) and $2\cdot34$ (calculated). The Θ values are about 10% below those of Fig. 4*a*, while the $\mathscr{M}$ values are much reduced, particularly at the smaller channel radii (e.g. $\mathscr{M} \approx 0\cdot09$, $0\cdot10$ for $a = 4\cdot5$, $5\cdot0$ fm). These values of $\mathscr{M}$ are in much better agreement with the shell model prediction (Fig. 6).

References

Ajzenberg-Selove, F. (1976). *Nucl. Phys.* A **268**, 1.
Andreev, G. B., Klyucharev, A. P., and Slabospitskii, R. P. (1973). *Izv. Akad. Nauk SSSR* (*ser. fiz.*) **37**, 183 (English transl.: *Bull. Acad. Sci. USSR* (*Phys. Ser.*) **37**, 160).
Armstrong, J. C., Baggett, M. J., Harris, W. R., and Latorre, V. A. (1966). *Phys. Rev.* **144**, 823.
Barker, F. C. (1961). *Nucl. Phys.* **28**, 96.
Barker, F. C. (1967). *Aust. J. Phys.* **20**, 341.
Barker, F. C. (1972). *Aust. J. Phys.* **25**, 341.
Barker, F. C. (1978). *Aust. J. Phys.* **31**, 27.
Bennett, L. A. (1976). Ph.D. Thesis, Australian National University.
Blatt, J. M., and Weisskopf, V. F. (1952). 'Theoretical Nuclear Physics' (Wiley: New York).
Blatt, S. L., Marolt, G. L., and Goss, J. D. (1974). *Phys. Rev.* C **10**, 1319.
Bloch, C. (1957). *Nucl. Phys.* **4**, 503.
Christy, R. F., and Duck, I. (1961). *Nucl. Phys.* **24**, 89.
Cohen, S., and Kurath, D. (1965). *Nucl. Phys.* **73**, 1.
Cohen, S., and Kurath, D. (1967). *Nucl. Phys.* A **101**, 1.
Darden, S. E., Sen, S., Hiddleston, H. R., Aymar, J. A., and Yoh, W. A. (1973). *Nucl. Phys.* A **208**, 77.

DeVries, R. M. (1973). *Phys. Rev.* C **8**, 951.
Faessler, A. (1965). *Nucl. Phys.* **65**, 329.
Feshbach, H., Peaslee, D. C., and Weisskopf, V. F. (1947). *Phys. Rev.* **71**, 145.
Fortune, H. T., Gray, T. J., Trost, W., and Fletcher, N. R. (1969). *Phys. Rev.* **179**, 1033.
Fowler, W. A., Lauritsen, C. C., and Lauritsen, T. (1948). *Rev. Mod. Phys.* **20**, 236.
Fox, G., Polchinski, J. G., Rolfs, C., and Tombrello, T. A. (1975). Charge symmetry for mirror γ-ray transitions in ^{13}N and ^{13}C. Caltech Lemon Aid Preprint LAP-144.
Franey, M. A., Lilley, J. S., and Phillips, W. R. (1979). *Nucl. Phys.* A **324**, 193.
Glover, R. N., and Jones, A. D. W. (1966). *Nucl. Phys.* **84**, 673.
Goldhammer, P., Hill, J. R., and Nachamkin, J. (1968). *Nucl. Phys.* A **106**, 62.
Gubler, H. P., Plattner, G. R., Sick, I., Traber, A., and Weiss, W. (1977). *Nucl. Phys.* A **284**, 114.
Heaton, H. T., Menke, J. L., Schrack, R. A., and Schwartz, R. B. (1975). *Nucl. Sci. Eng.* **56**, 27.
Hebbard, D. F., and Vogl, J. L. (1960). *Nucl. Phys.* **21**, 652.
Holt, R. J., Jackson, H. E., Laszewski, R. M., Monahan, J. E., and Specht, J. R., (1978). *Phys. Rev.* C **18**, 1962.
Jackson, H. L., and Galonsky, A. I. (1953). *Phys. Rev.* **89**, 370.
Jäger, H. U., Kissener, H. R., and Eramzhian, R. A. (1971). *Nucl. Phys.* A **171**, 16.
Kane, J. V., Pixley, R. E., and Wilkinson, D. H. (1960). *Philos. Mag.* **5**, 365.
Karban, O., *et al.* (1976). *Nucl. Phys.* A **269**, 312.
Koester, L., and Nistler, W. (1975). *Z. Phys.* A **272**, 189.
Kurath, D. (1975). *Phys. Rev. Lett.* **35**, 1546.
Lachkar, J. C. (1977). Proc. Int. Specialists Symp. on Neutron Standards and Applications, Gaithersburg, Maryland, March 28–31, 1977. NBS Special Publication No. 493, p. 93.
Lane, A. M. (1960). *Rev. Mod. Phys.* **32**, 519.
Lane, A. M., and Robson, D. (1966). *Phys. Rev.* **151**, 774.
Lane, A. M., and Thomas, R. G. (1958). *Rev. Mod. Phys.* **30**, 257.
Ludwig, E. J., Busch, C. E., Clegg, T. B., Datta, S. K., and Watkins, A. C. (1974). *Nucl. Phys.* A **230**, 271.
Marrs, R. E., Adelberger, E. G., Snover, K. A., and Cooper, M. D. (1975). *Phys. Rev. Lett.* **35**, 202.
Nair, K. G., *et al.* (1975). *Phys. Rev.* C **12**, 1575.
Nair, K. G., Voit, H., Hamm, M., Towsley, C., and Nagatani, K. (1974). *Phys. Rev. Lett.* **33**, 1588.
Pearson, C. A., *et al.* (1972). *Nucl. Phys.* A **191**, 1.
Riess, F., Paul, P., Thomas, J. B., and Hanna, S. S. (1968). *Phys. Rev.* **176**, 1140.
Robinson, S. W., Swann, C. P., and Rasmussen, V. K. (1968). *Phys. Lett.* B **26**, 298.
Rolfs, C. (1973). *Nucl. Phys.* A **217**, 29.
Rolfs, C., and Azuma, R. E. (1974). *Nucl. Phys.* A **227**, 291.
Schiffer, J. P., Morrison, G. C., Siemssen, R. H., and Zeidman, B. (1967). *Phys. Rev.* **164**, 1274.
Seagrave, J. D. (1951). *Phys. Rev.* **84**, 1219.
Seagrave, J. D. (1952). *Phys. Rev.* **85**, 197.
Shlomo, S. (1978). *Rep. Prog. Phys.* **41**, 957.
Taketani, H., Muto, J., Yamaguchi, H., and Kokame, J. (1968). *Phys. Lett.* B **27**, 625.
Thomas, R. G. (1952). *Phys. Rev.* **88**, 1109.
Tombrello, T. A., and Parker, P. D. (1963). *Phys. Rev.* **131**, 2582.
Tryti, S., Holtebekk, T., and Ugletveit, F. (1975). *Nucl. Phys.* A **251**, 206.
Van Patter, D. M. (1949). *Phys. Rev.* **76**, 1264.
Varma, S., and Goldhammer, P. (1969). *Nucl. Phys.* A **125**, 193.
Vogl, J. L. (1963). Ph.D. Thesis, California Institute of Technology.
Von Oertzen, W., and Bohlen, H. G. (1975). *Phys. Rep.* **19**, 1.
Warburton, E. K., Alburger, D. E., and Milliner, D. J. (1980). *Phys. Rev.* C **22**, 2330.
Warburton, E. K., and Weneser, J. (1969). *In* 'Isospin in Nuclear Physics' (Ed. D. H. Wilkinson), p. 173 (North-Holland: Amsterdam).
Woodbury, H. H., Tollestrup, A. V., and Day, R. B. (1954). *Phys. Rev.* **93**, 1311.
Young, F. C., Armstrong, J. C., and Marion, J. B. (1963). *Nucl. Phys.* **44**, 486.
Zeller, A. F., *et al.* (1979). *Nucl. Phys.* A **323**, 477.

Manuscript received 10 December 1979, accepted 21 February 1980